Synthetic Aperture Microwave Imaging on MAST and NSTX-U

S. J. Freethy[1], K. J. Brunner[1,2] , J Chorley[1,2] D. Thomas[1,3], V. F. Shevchenko[1], J. Urban[4] and R. G. L. Vann[3]

1 EURATOM/CCFE Fusion Association, Abingdon, Oxfordshire, OX14 3DB, UK
2 Centre for Advanced Instrumentation, Department of Physics, Durham University, Durham, UK
3 York Plasma Institute Department of physics, University of York, York, YO10 5DD, UK
4 Institute of Plasma Physics, Academy of Sciences of the Czech Republic, Prague

Outline

- Introduction and motivations – S. J. Freethy
  - Introduction to SAMI
  - Introduction to EBW emission
  - Results from MAST
- Reflectometry and backscattering – D. Thomas
  - Multiple reflectometers
  - Backscattering and Doppler shifts
- Technical developments and upgrade – J. Brunner
  - FPGAs
  - The SAMI digitiser
  - FPGA/GPU data “real-time” data processing

Outline

- Introduction and motivations – S. J. Freethy
  - Introduction to SAMI
  - Introduction to EBW emission
  - Results from MAST
- Reflectometry and backscattering – D. Thomas
  - Multiple reflectometers
  - Backscattering and Doppler shifts
- Technical developments and upgrade – J. Brunner
  - FPGAs
  - The SAMI digitiser
  - FPGA/GPU data “real-time” data processing

Research Councils UK Energy For a Low Carbon Future
EPSRC Engineering and Physical Sciences Research Council
UNIVERSITY of York
Durham University
CCFE CULHAM CENTRE FOR FUSION ENERGY

SAMI is a thinned array

For imaging microwaves you can use…

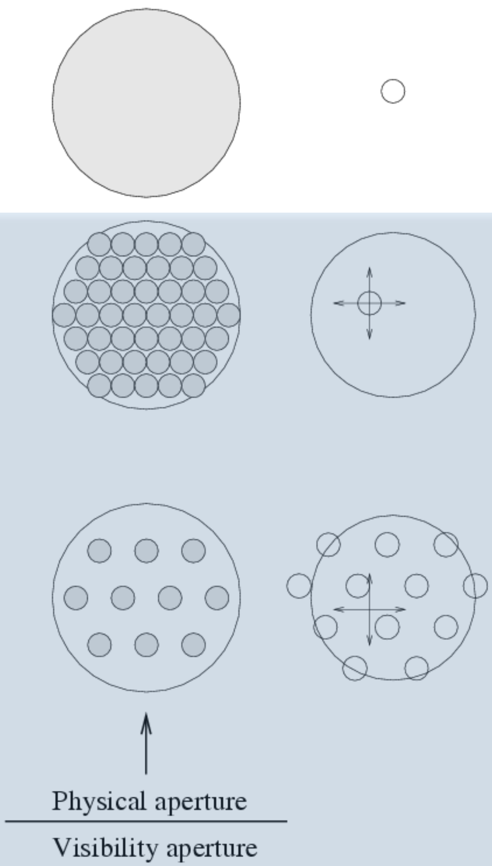

- A lens or mirror element steered by moving the element,
- or used to focus image onto an array of detectors.

- A traditional phased array is a filled aperture of phase sensitive antennas.
- Beam is steered through phase control of elements
- High signal to noise, but high redundancy

- A thinned array makes use of the spatial incoherence of the source to remove redundancies, making images of the same fidelity with much fewer elements
- Beam is steered through phase control of elements
- Beam steering replaced by Fourier Transform

SAMI is a thinned array

For imaging microwaves you can use…

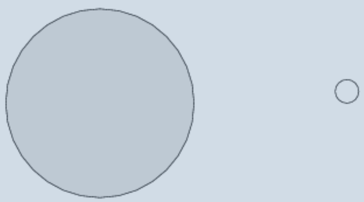

- A lens or mirror element steered by moving the element,
- or used to focus image onto an array of detectors.

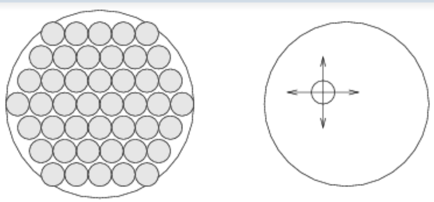

- A traditional phased array is a filled aperture of phase sensitive antennas.
- Beam is steered through phase control of elements
- High signal to noise, but high redundancy

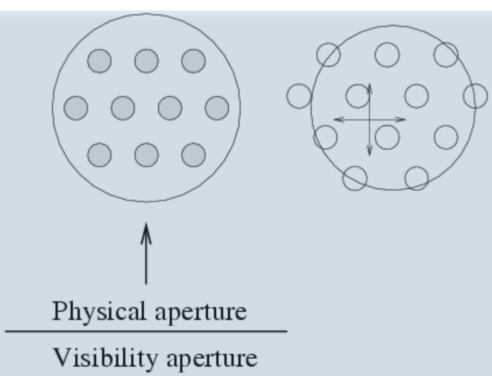

- A thinned array makes use of the spatial incoherence of the source to remove redundancies, making images of the same fidelity with much fewer elements
- Beam is steered through phase control of elements
- Beam steering replaced by Fourier Transform

SAMI is a thinned array

For imaging microwaves you can use…

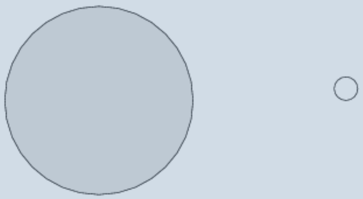

- A lens or mirror element steered by moving the element,
- or used to focus image onto an array of detectors.

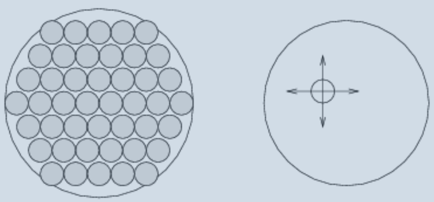

- A traditional phased array is a filled aperture of phase sensitive antennas.
- Beam is steered through phase control of elements
- High signal to noise, but high redundancy

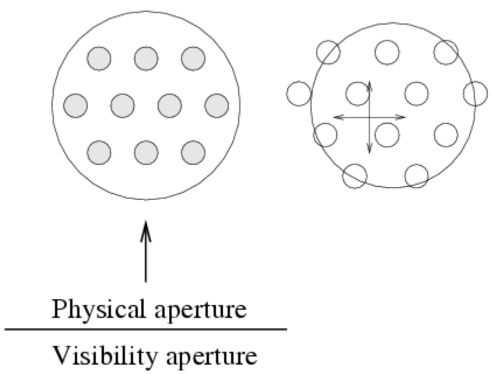

- A thinned array makes use of the spatial incoherence of the source to remove redundancies, making images of the same fidelity with much fewer elements
- Beam is steered through phase control of elements
- Beam steering replaced by Fourier Transform

SAMI array

8 Antenna array installed on MAST

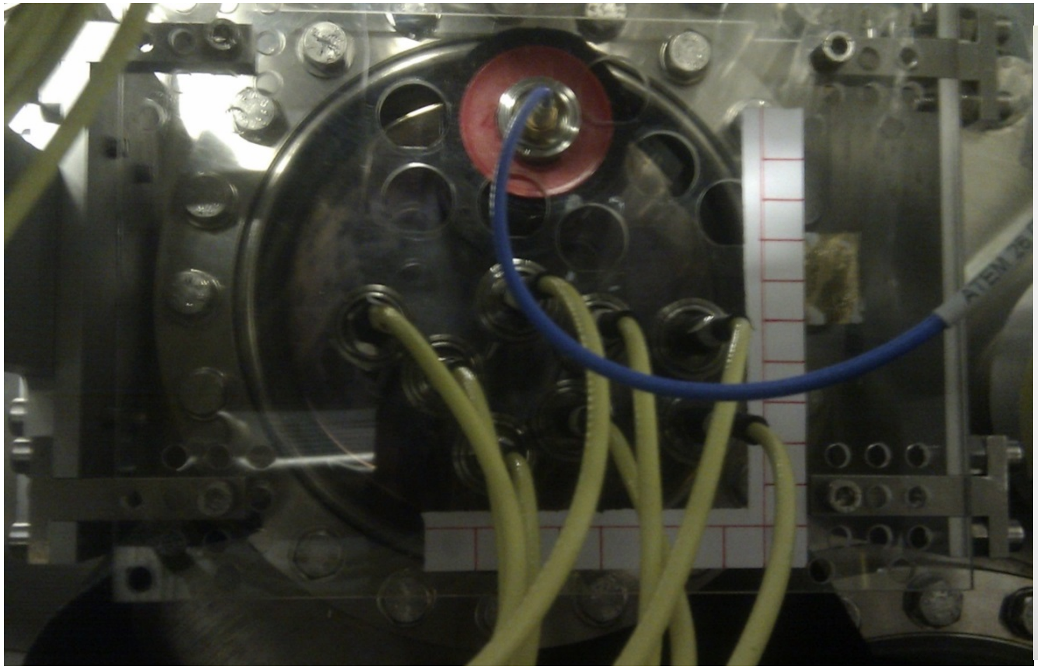

36 Antenna array for illustration

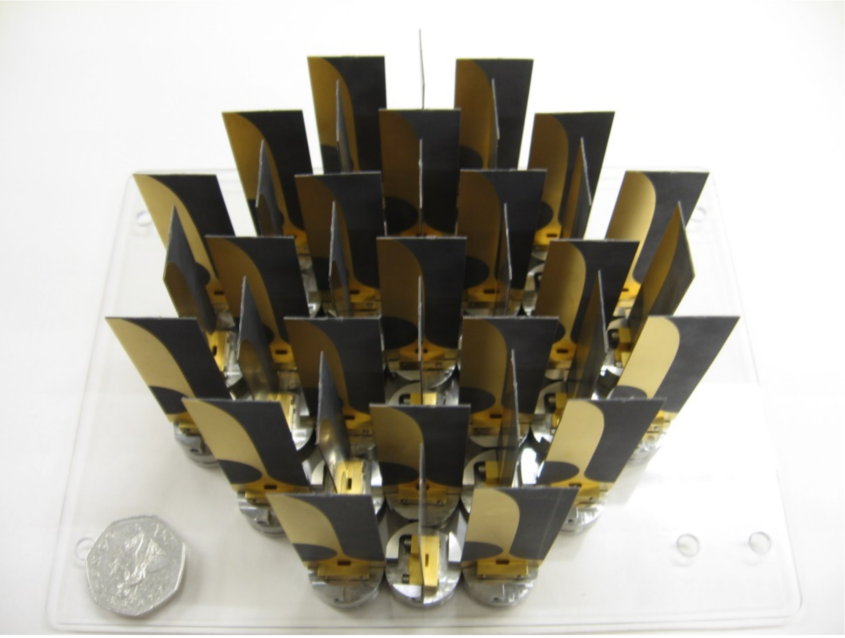

Linear polarised, very broadband PCB based antenna

Array has wide field of view -> small antenna spacings

Emission from over-dense machines

- Most conventional tokamaks emit thermal radiation from Cyclotron harmonics
- High beta machines tend to have their harmonics covered by cut-offs

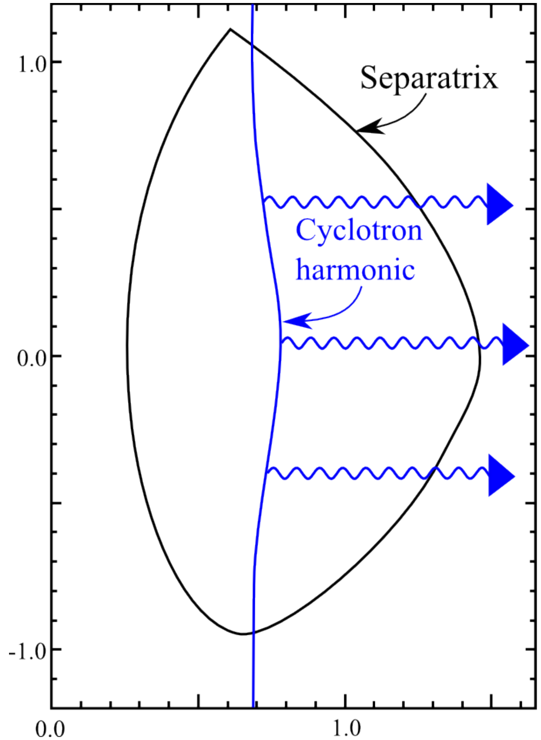

Under-dense -> Normal ECE

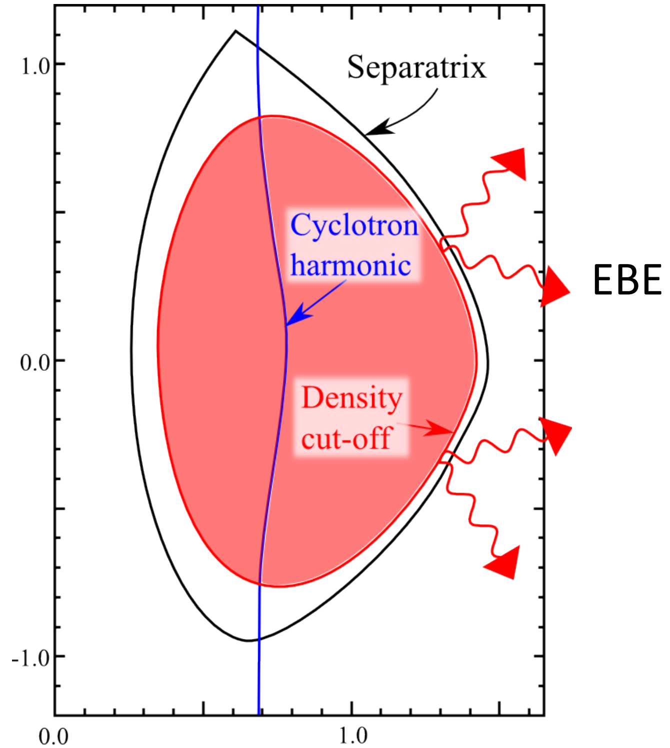

Over-dense -> mode converted emission

Mode converted emission

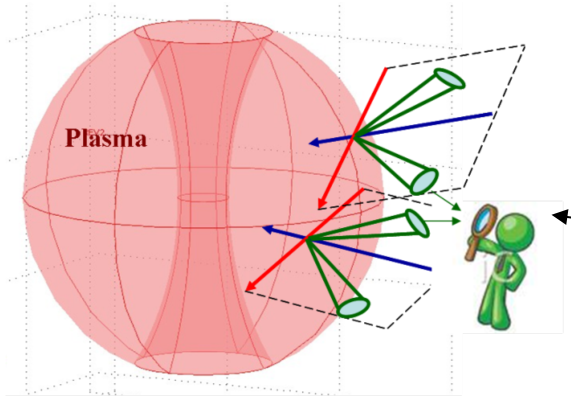

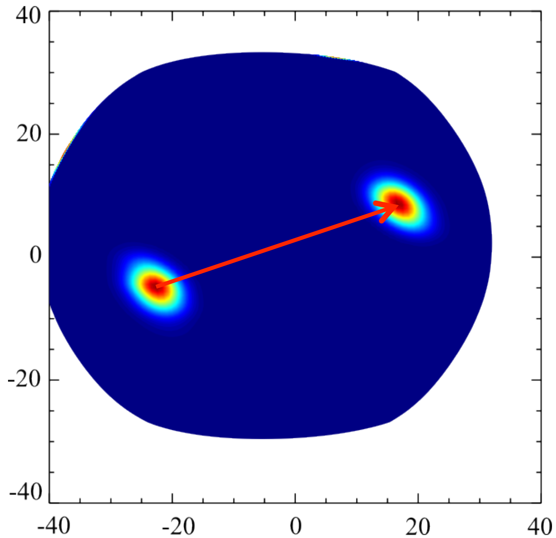

• The dependence of the Mode Conversion (MC) on the incident angle to the field means the emission is anisotropic.

• The MC'd emission takes the form of narrow angular cones.

• When all emission is considered, it appears as two spots on the plasma density surface along the magnetic field line.

• Mode conversion happens at different layers in the plasma for different frequencies, so we may diagnose different radii

Mode Converted Emission

- The brightness-temperature of the emission is the product of the brightness-temperature of the EBW at source and the mode conversion coefficient.

$$T_{obs} = T_{EBE}\,\tau_{mc}$$

Ray tracing shows strong off-midplane Doppler broadening

11GHz example – Only rays on the midplane originate at the cyclotron harmonic

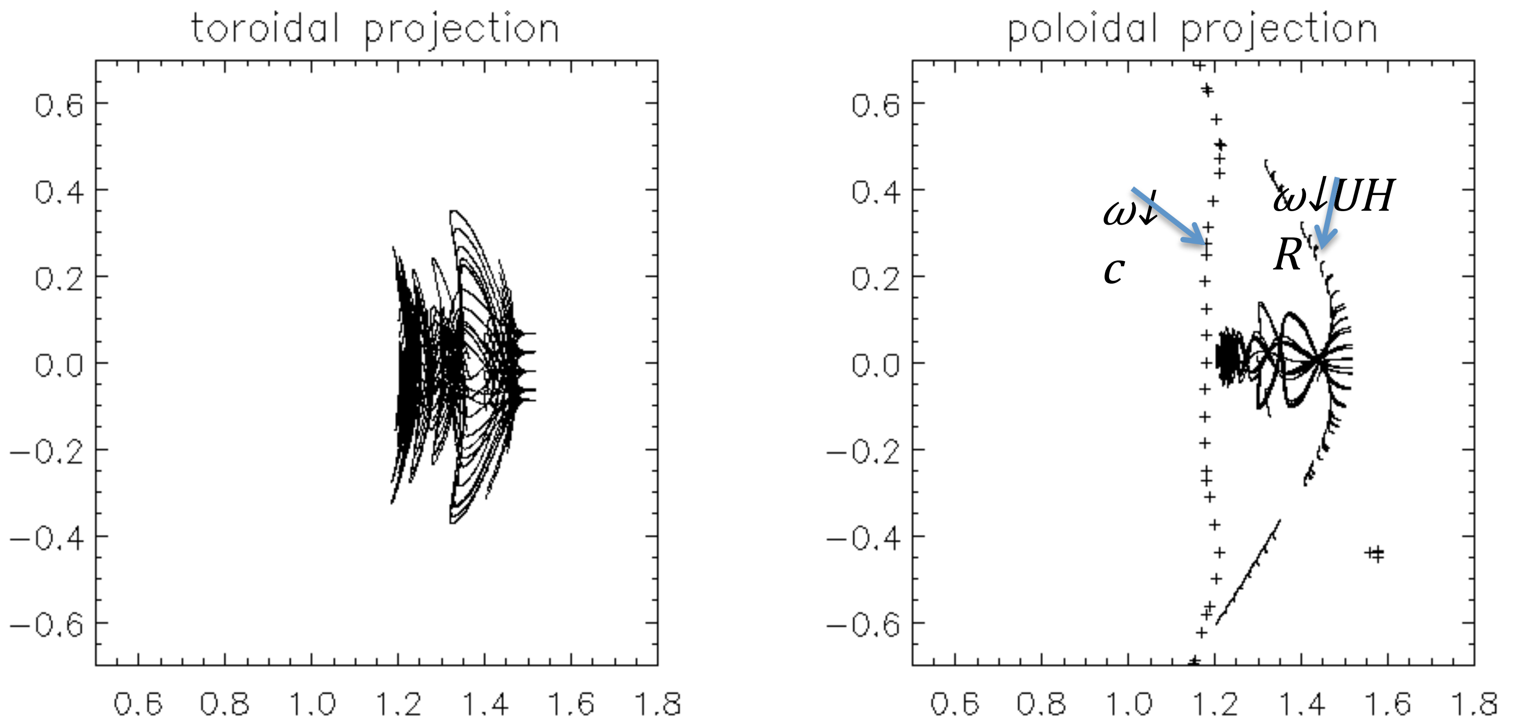

Off midplane, the rays originate from the colder outer regions

Maximum penetration between harmonics

15GHz example – Maximum penetration of ***off midplane*** rays happens between harmonics

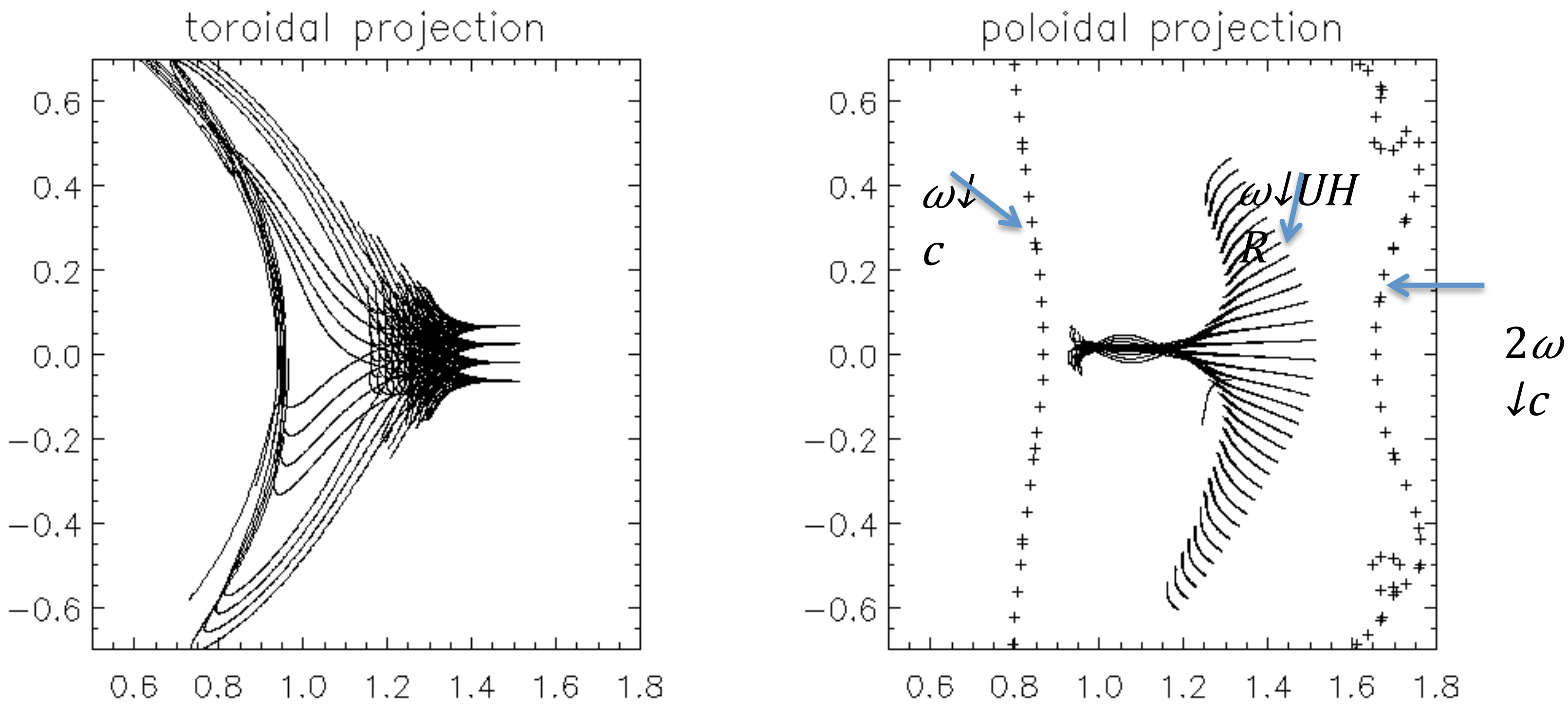

Radiative temperature effect

Performing AMR simulations we can see that, for low frequencies, the wave refraction dominates the observable emission profile.

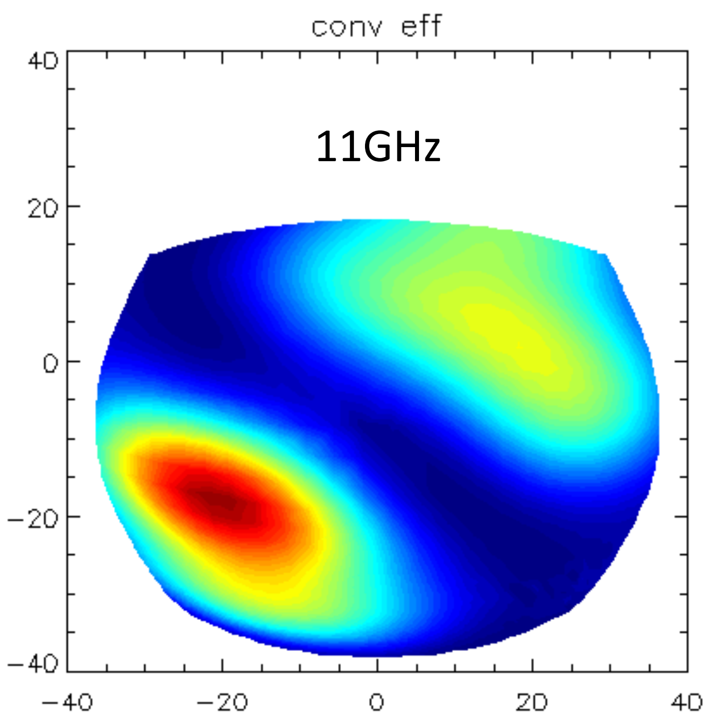

X

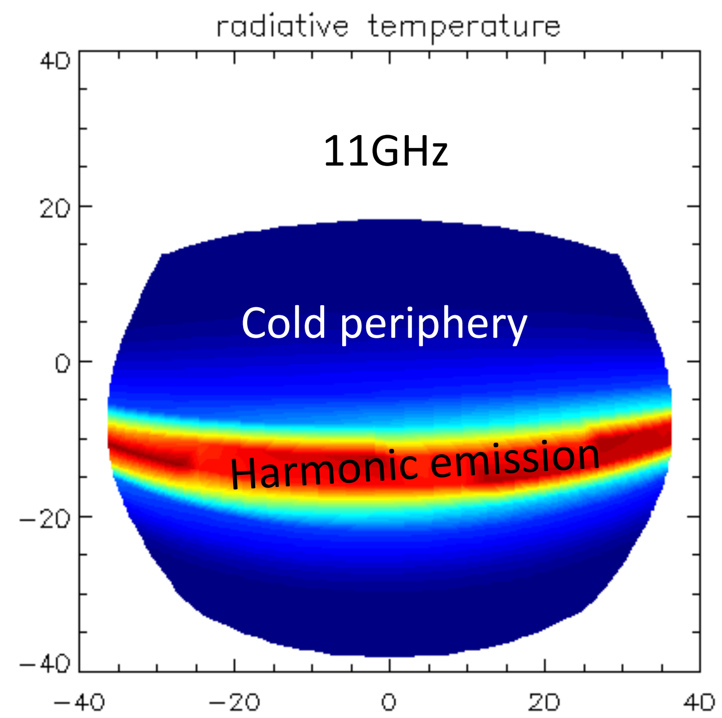

Research Councils UK Energy For a Low Carbon Future
EPSRC Engineering and Physical Sciences Research Council
UNIVERSITY of York
Durham University
CCFE CULHAM CENTRE FOR FUSION ENERGY

Radiative temperature effect

In between the harmonics, the effect is less pronounced, but still present.

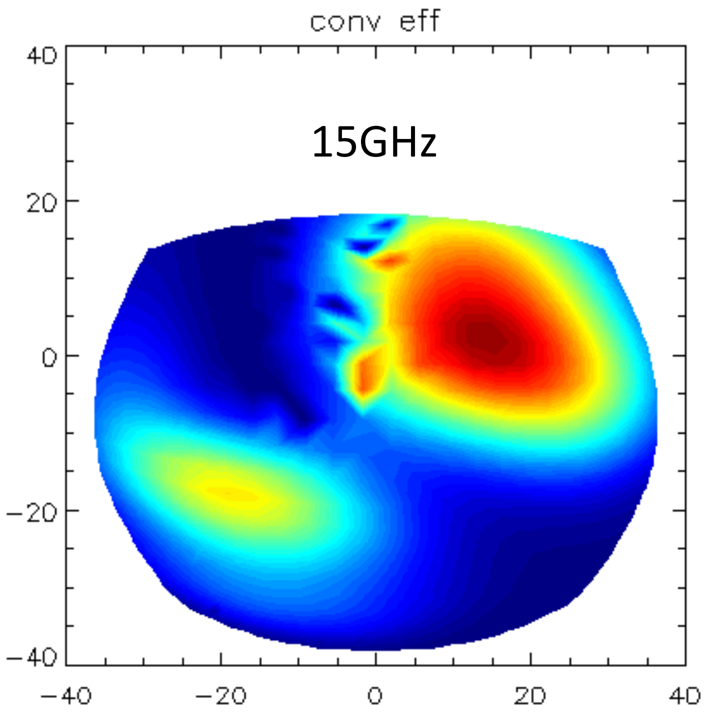

X

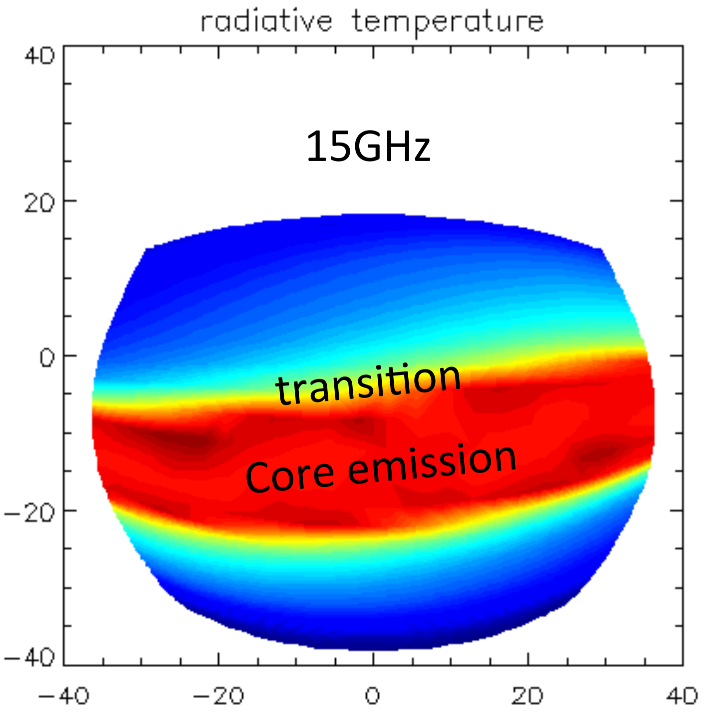

Forward model 11GHz

Excellent agreement between convolved AMR emission and observed emission

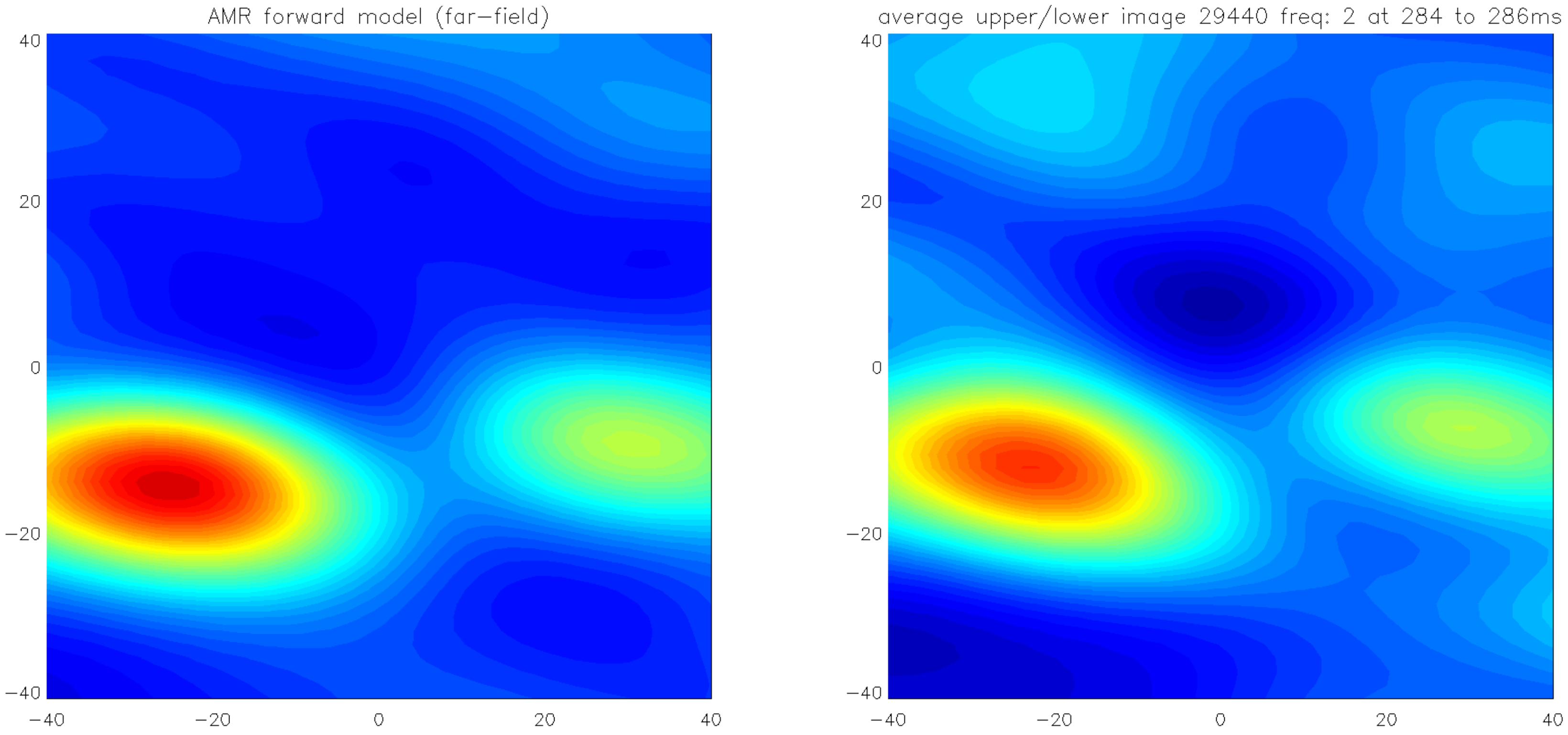

Research Councils UK Energy For a Low Carbon Future
EPSRC Engineering and Physical Sciences Research Council
UNIVERSITY of York
Durham University
CCFE CULHAM CENTRE FOR FUSION ENERGY

Forward model 15GHz

Less good agreement at higher frequencies.
"Pitch" is consistently flatter than predicted

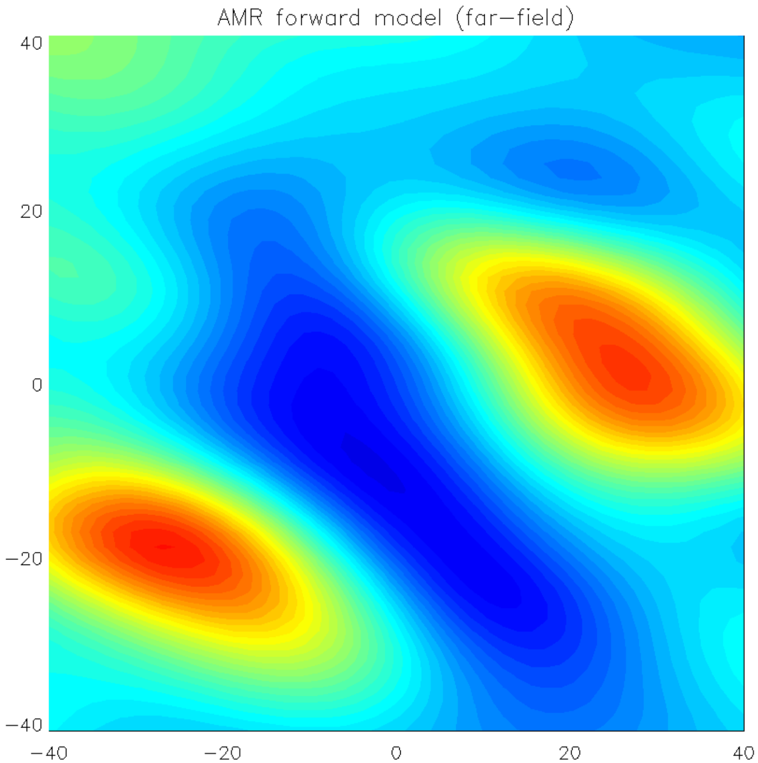

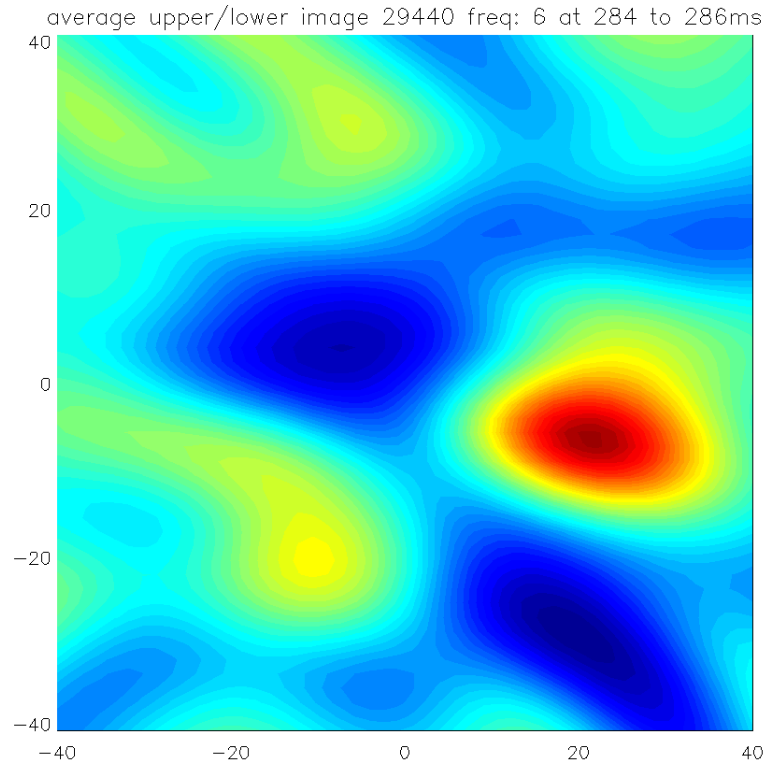

Forward model 16GHz

Elongation of observed upper window, due to emission window splitting in two

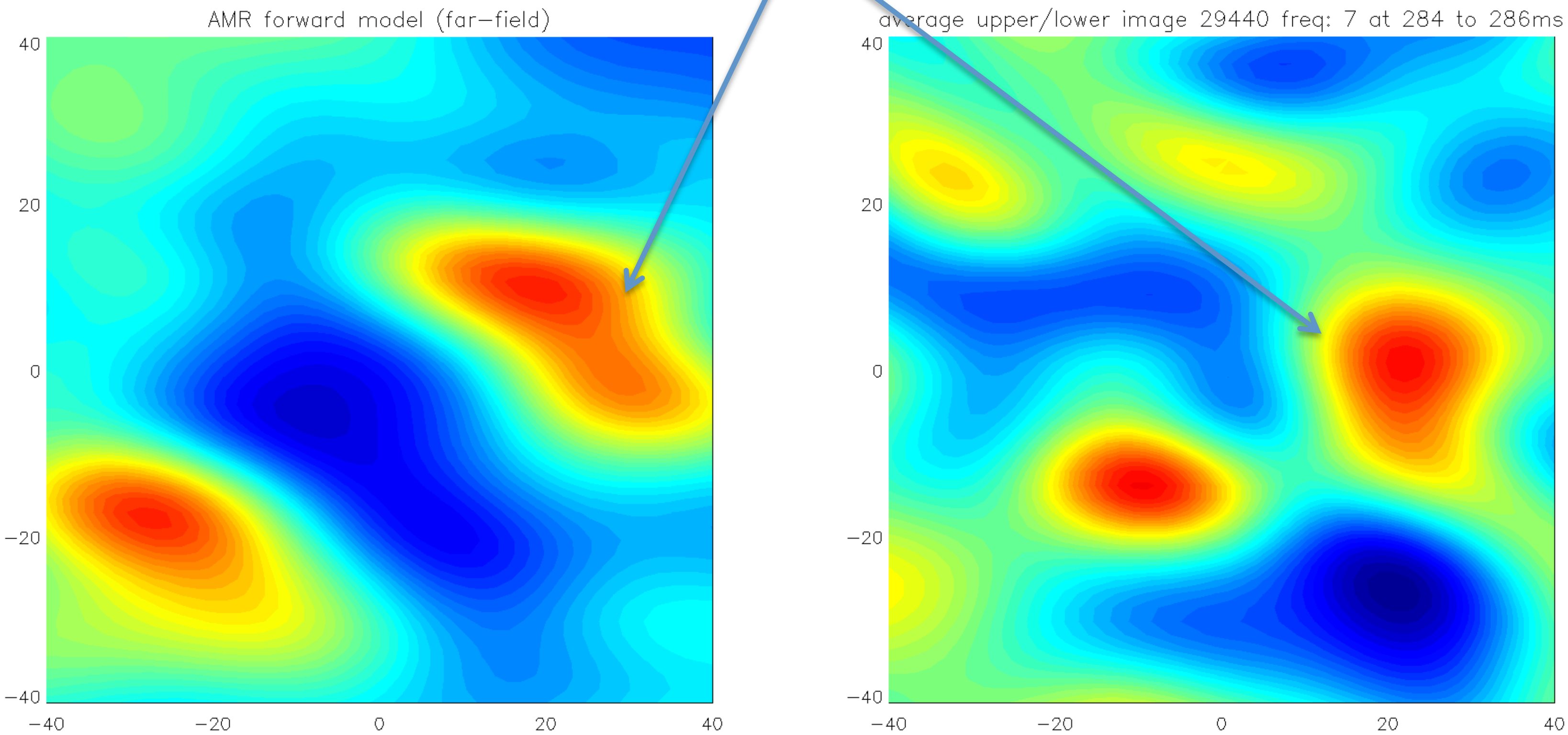

Forward model 17GHz

Right hand window moves up off the midplane signalling 2nd harmonic emission beginning to take over. Hotter, fundamental emission is seen only off midplane.

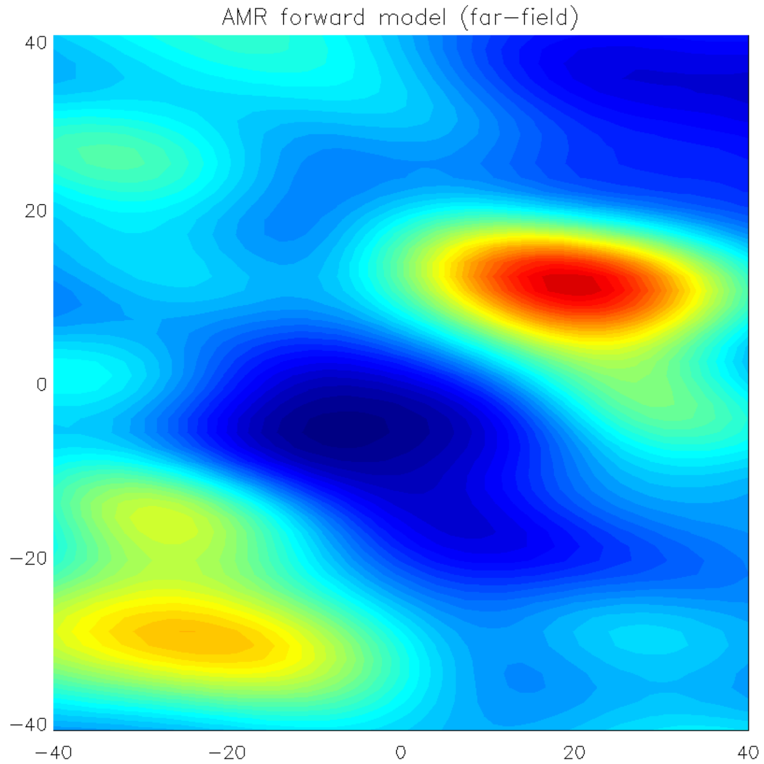

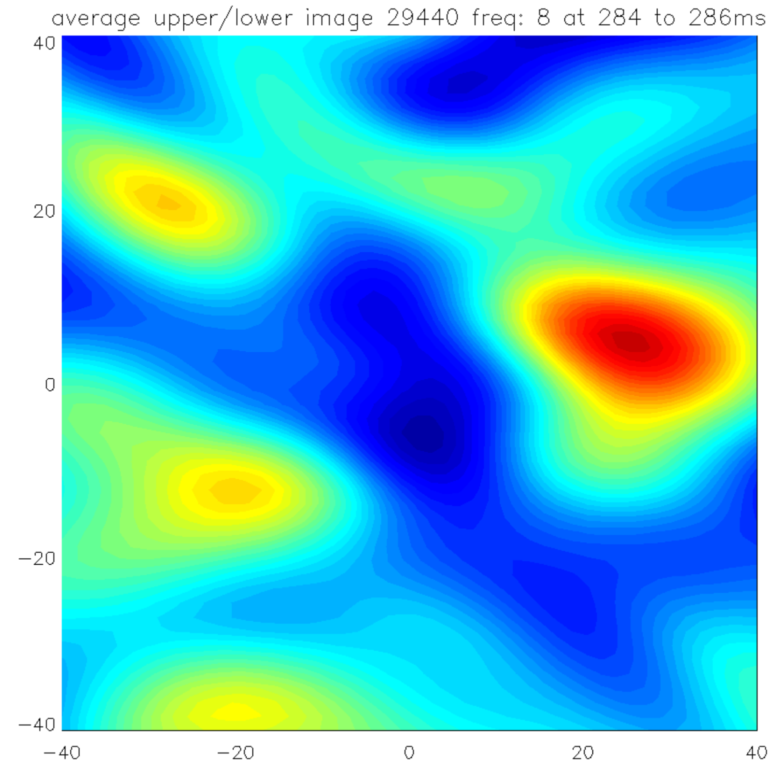

Forward model 18GHz

Continuing to higher frequencies, the midplane emission shuts down entirely as the 2nd harmonic begins to overlap with the UHR

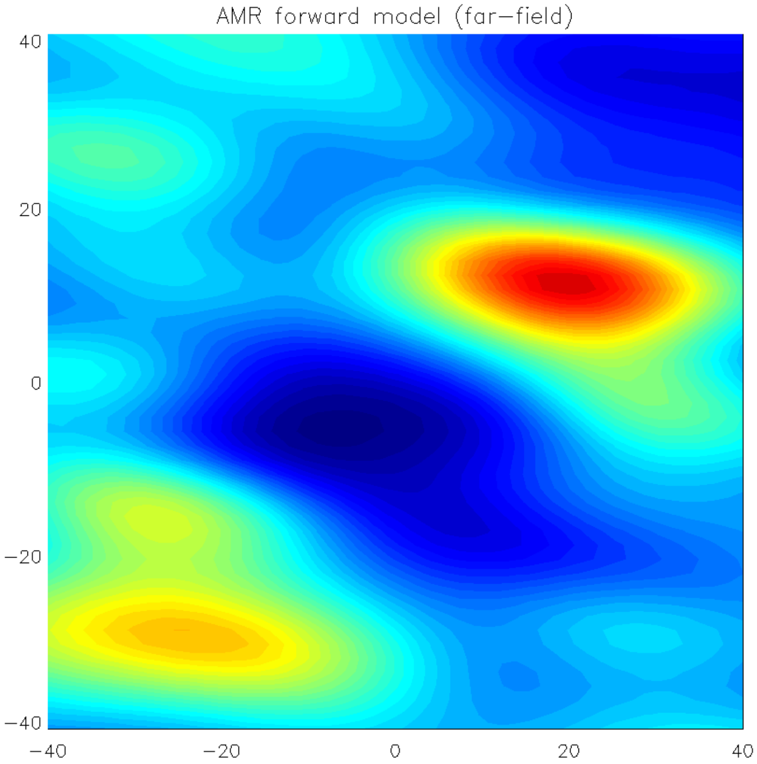

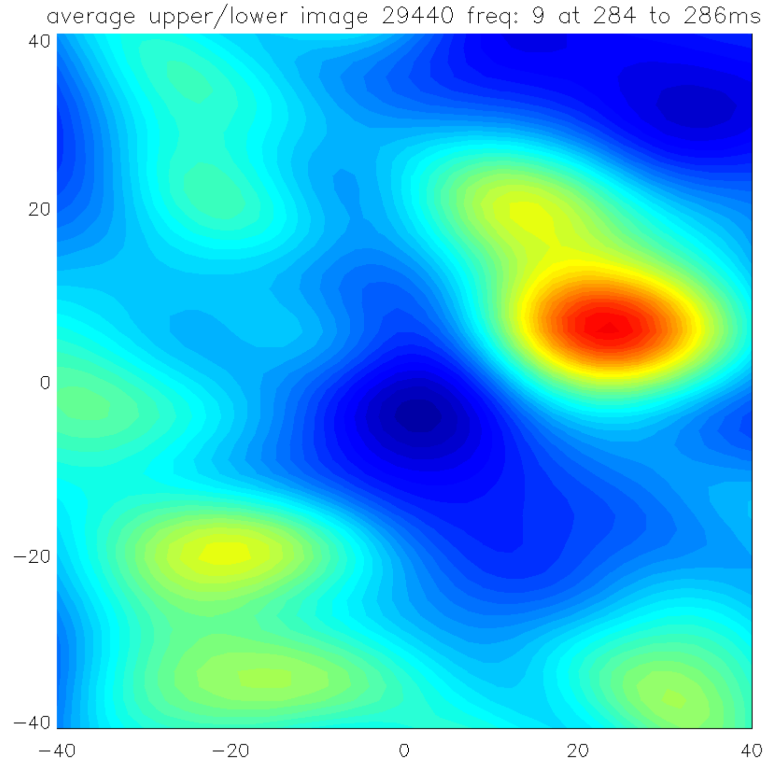

Density dependence of emission

Scooped lower frequencies

Peak emission moves to higher frequency

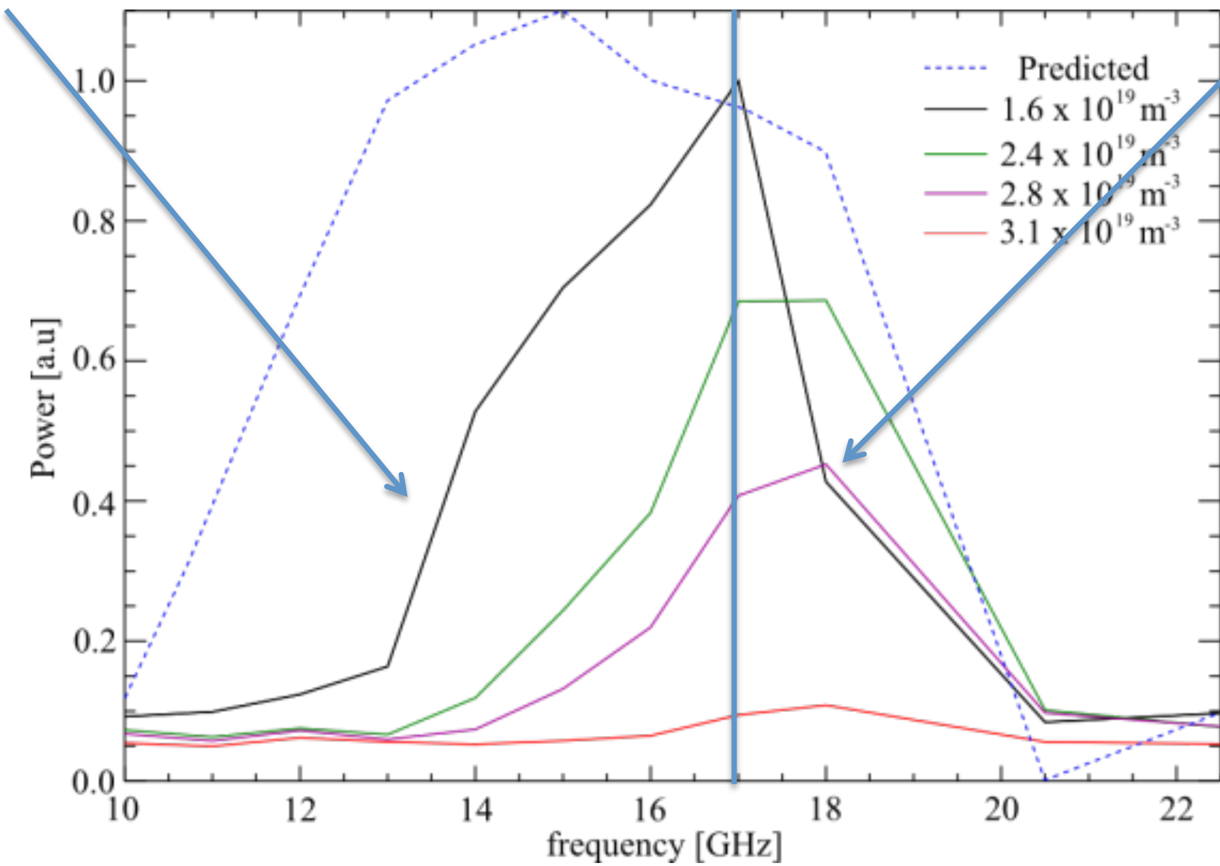

Array on midplane
ne = 1.6e19 m^{-1}

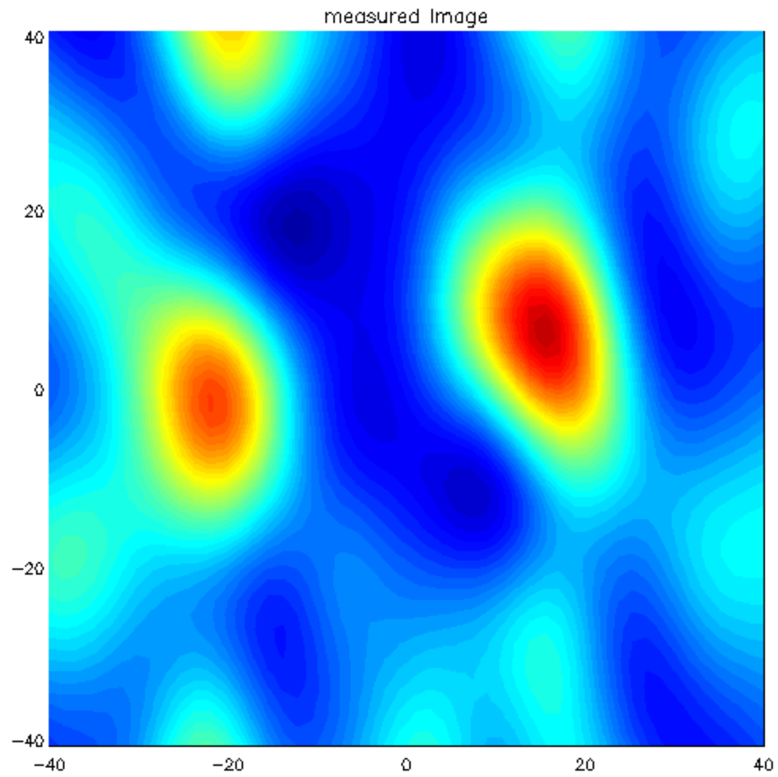

Clear trend of decreasing apparent pitch with increasing ne.

Array on midplane
ne = 2.4e19 m^{-1}

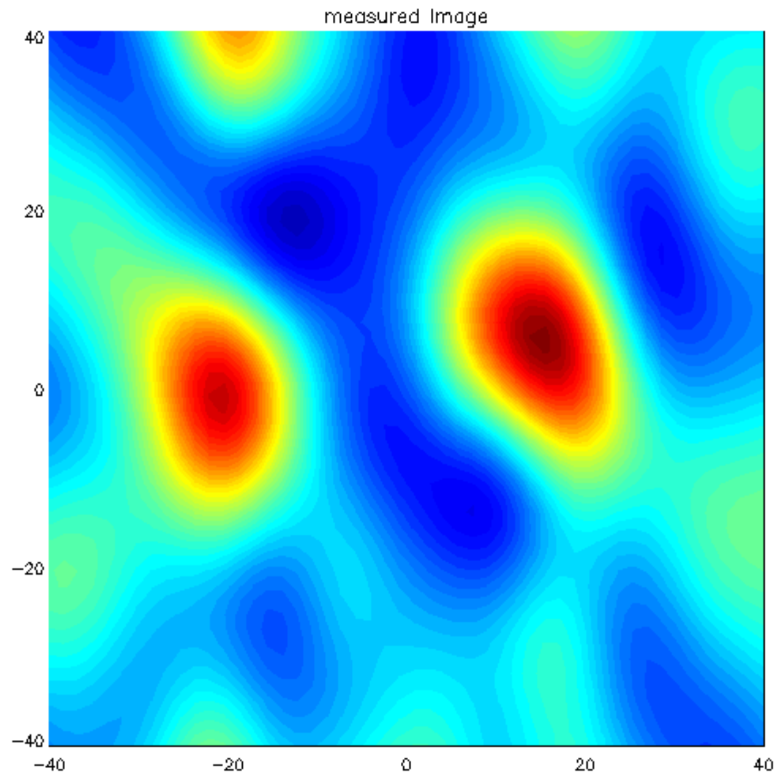

Clear trend of decreasing apparent pitch with increasing ne.

Array on midplane ne = 2.8e19 m^{-1}

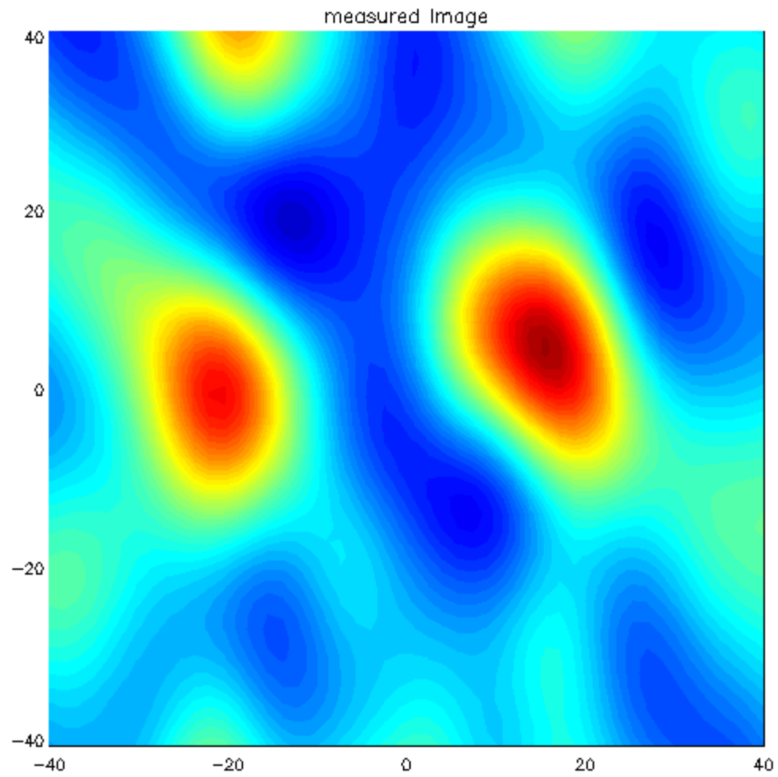

Clear trend of decreasing apparent pitch with increasing ne.

Array on midplane
ne = 3.1e19 m^{-1}

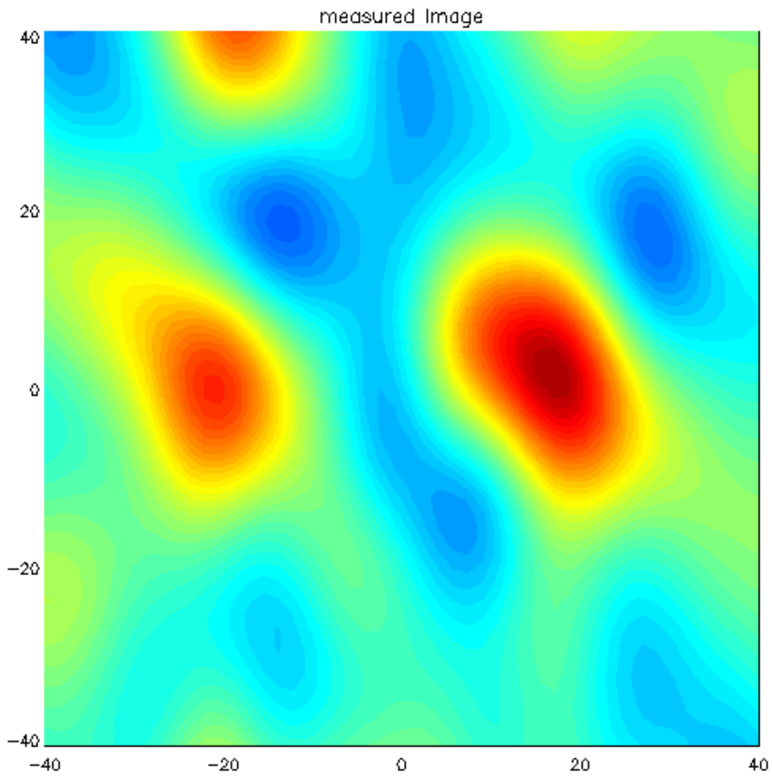

Clear trend of decreasing apparent pitch with increasing ne.

Single antenna setups

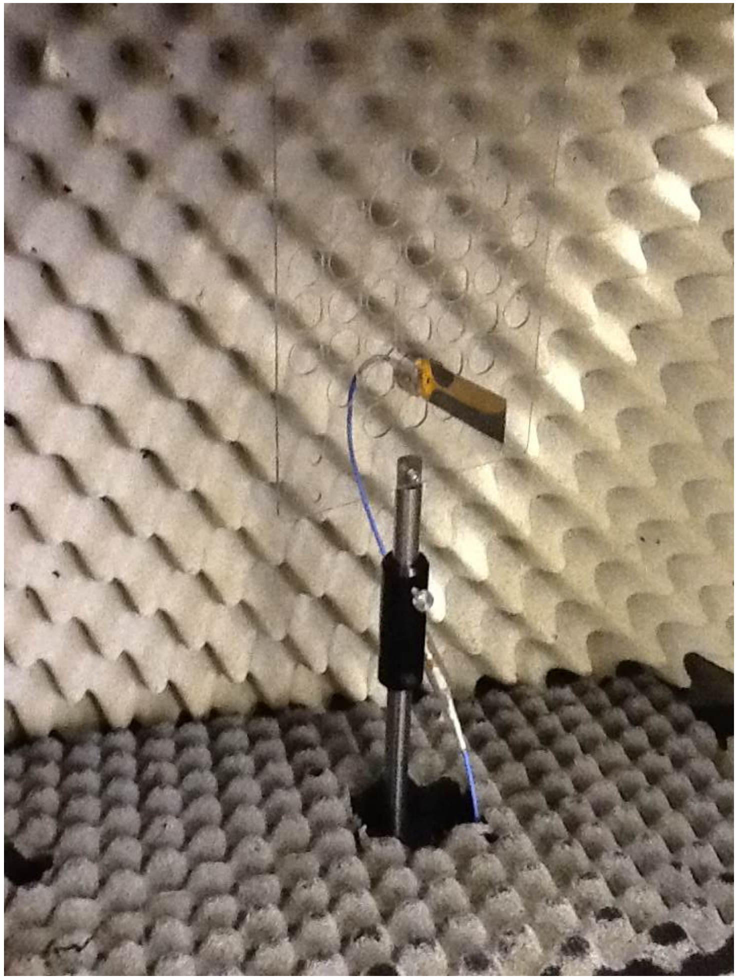

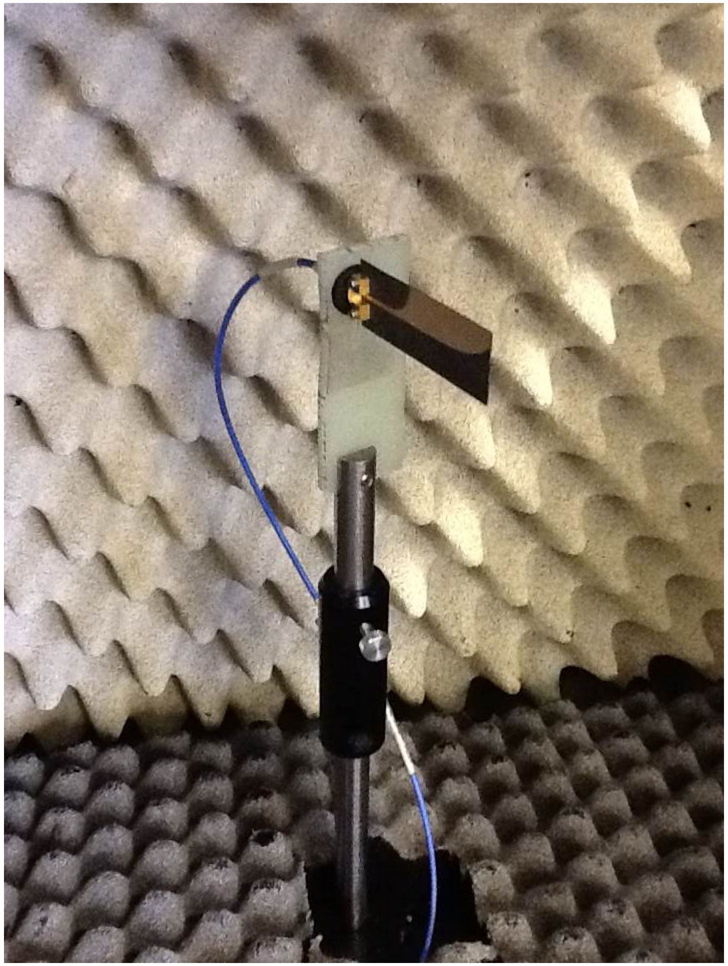

Normalised straight ahead and power in dB

Colour range = -15dB – >5 dB

With holder

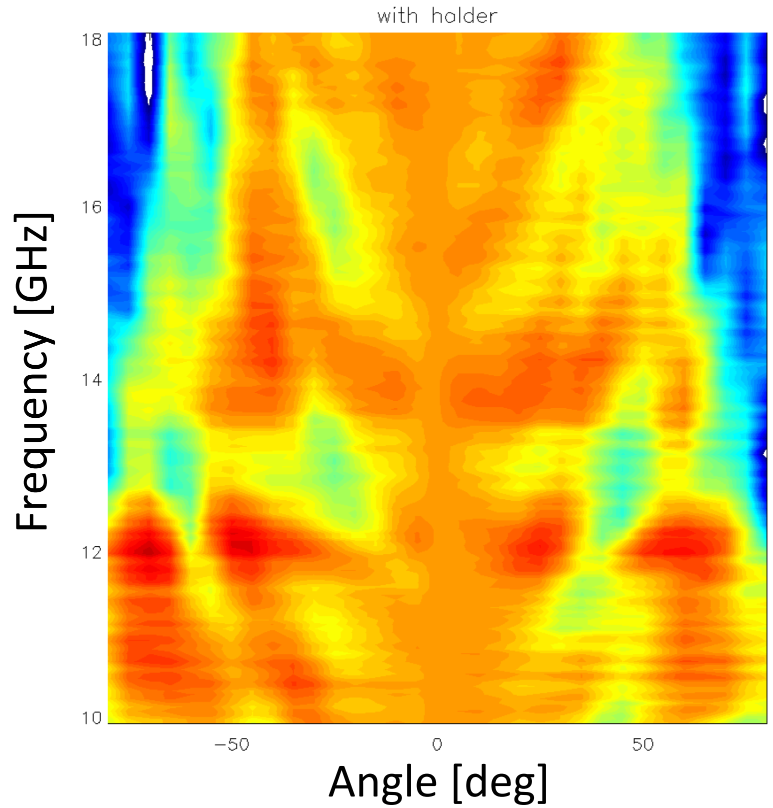

No holder

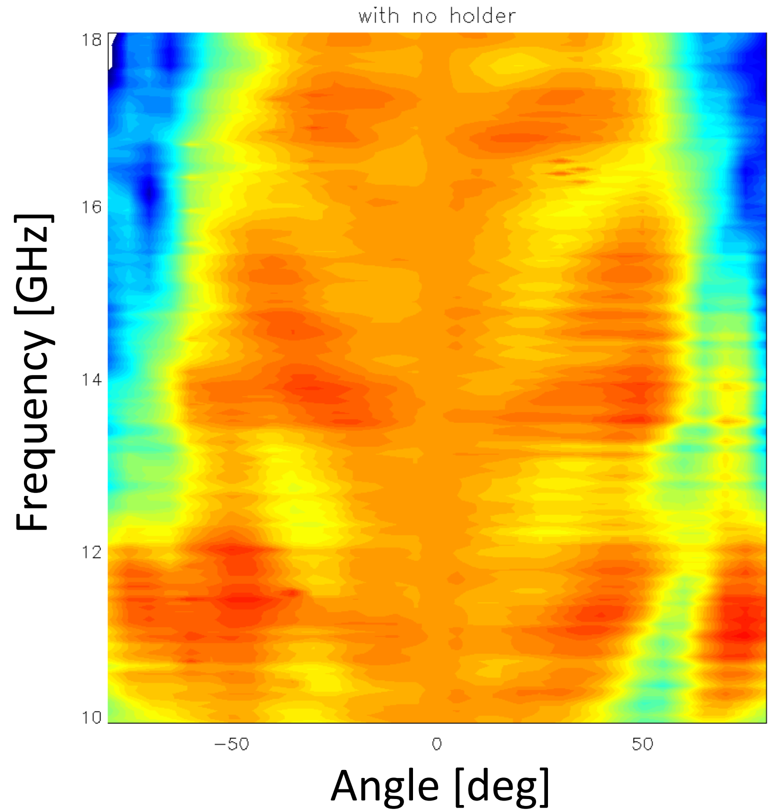

Antenna comparisons

Colour range = -15dB – >5 dB

Antenna 4 in array

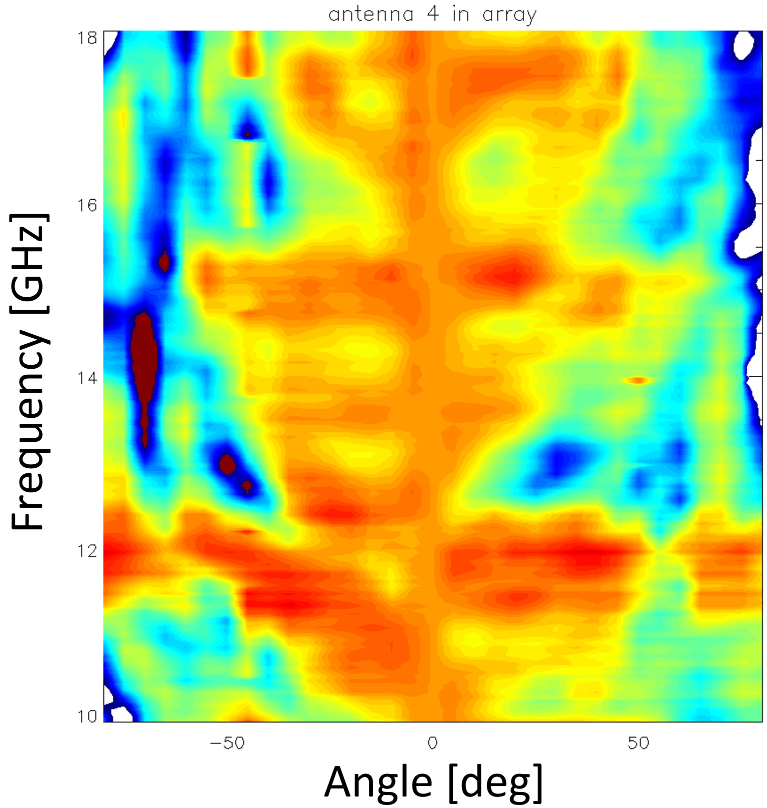

Single antenna

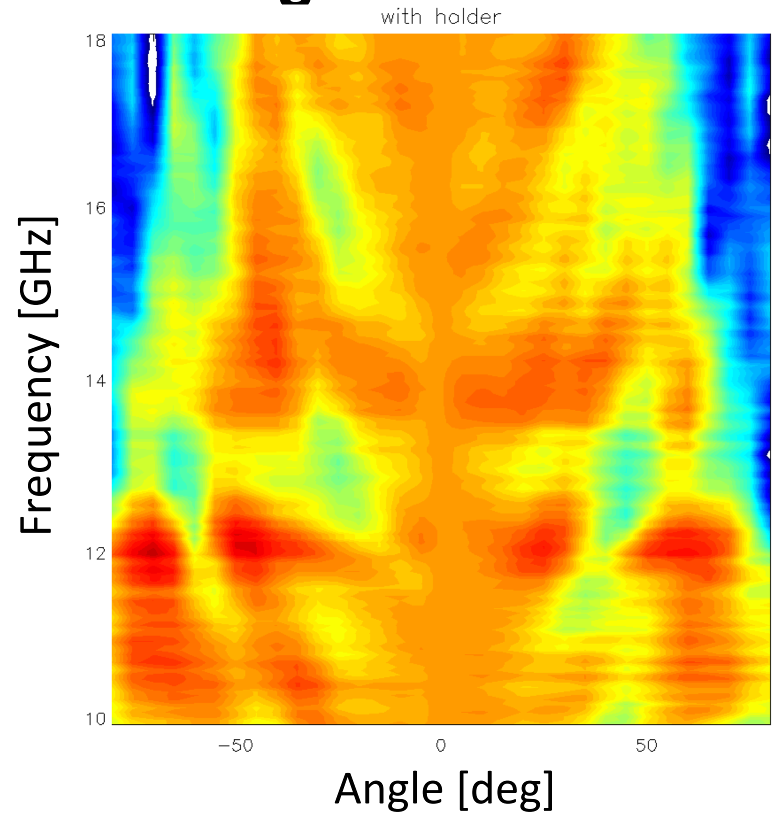

3D array effects distort antenna beam patterns

- The presence of other antennas distorts the beam pattern.
- The antenna cross talk is too low to be causing the issue.
- A full wave model of the array is required to diagnose and correct the problem.
- We perform modelling using a commercial package called COMSOL.

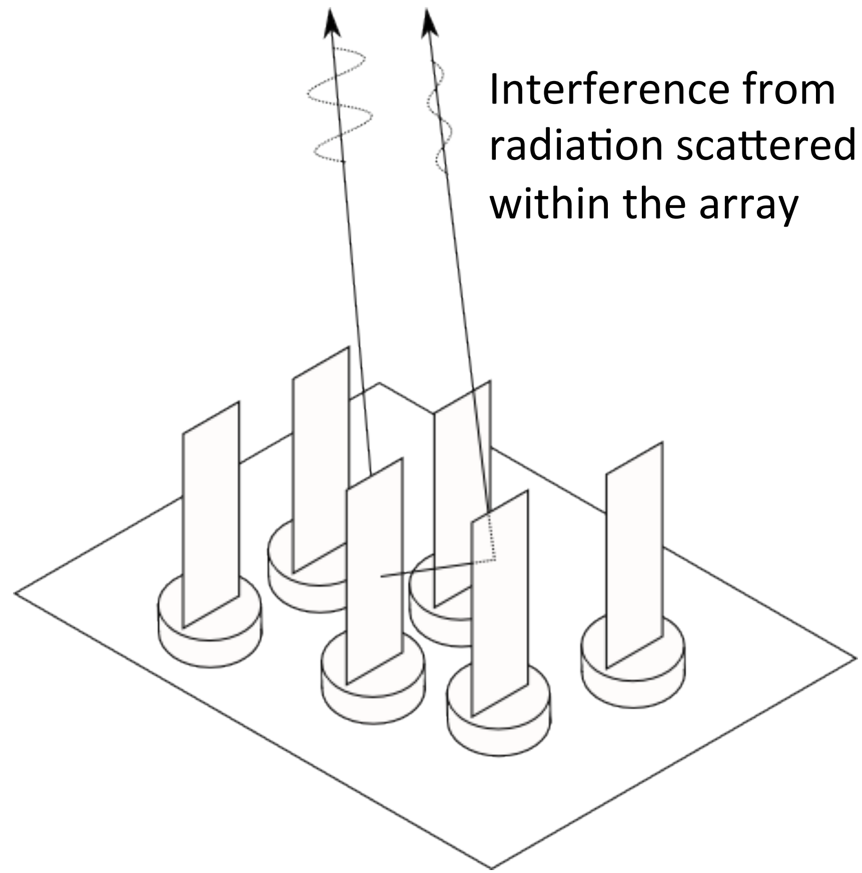

Array modelling

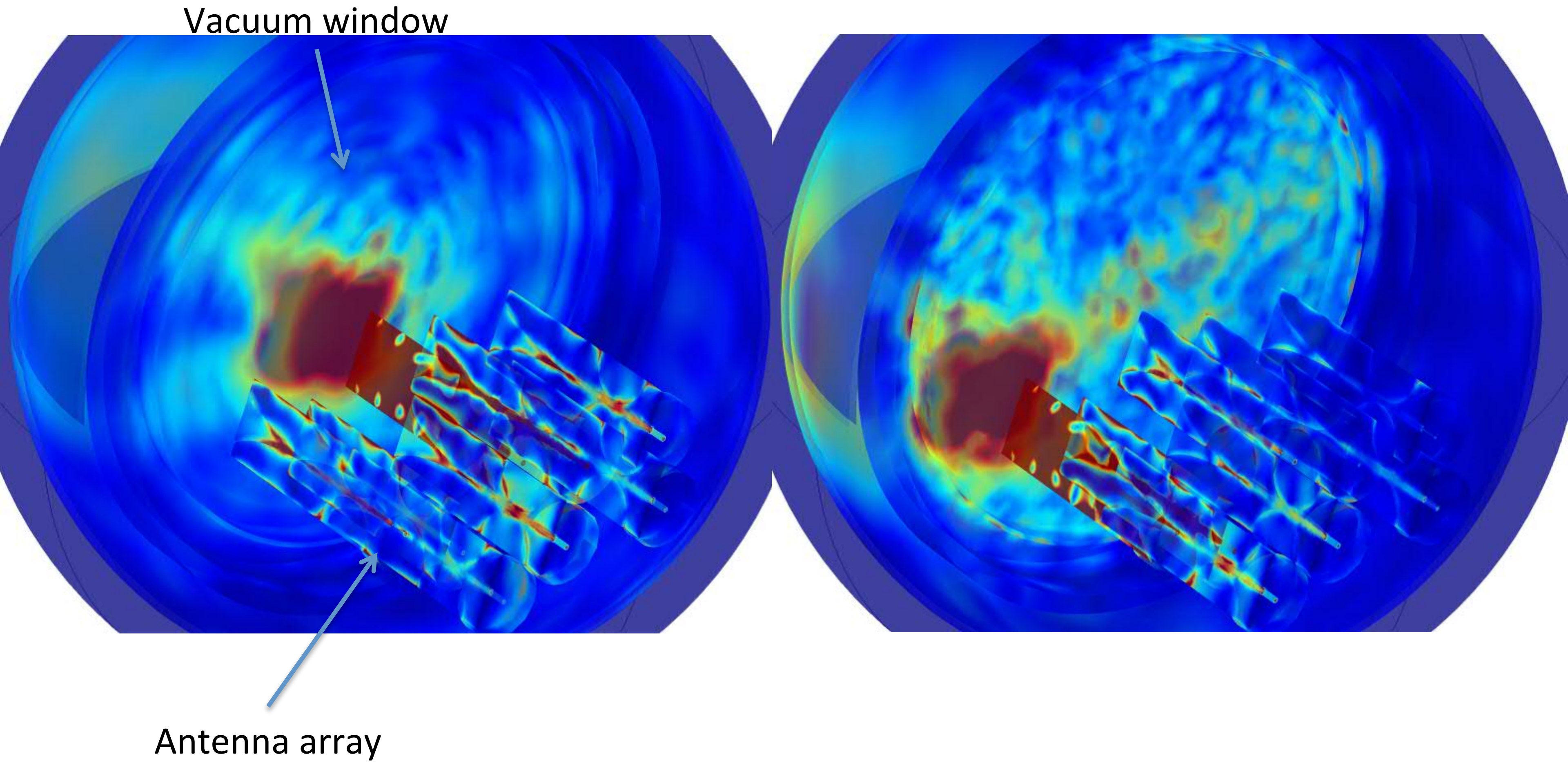

Full wave extrapolation to measurement domain

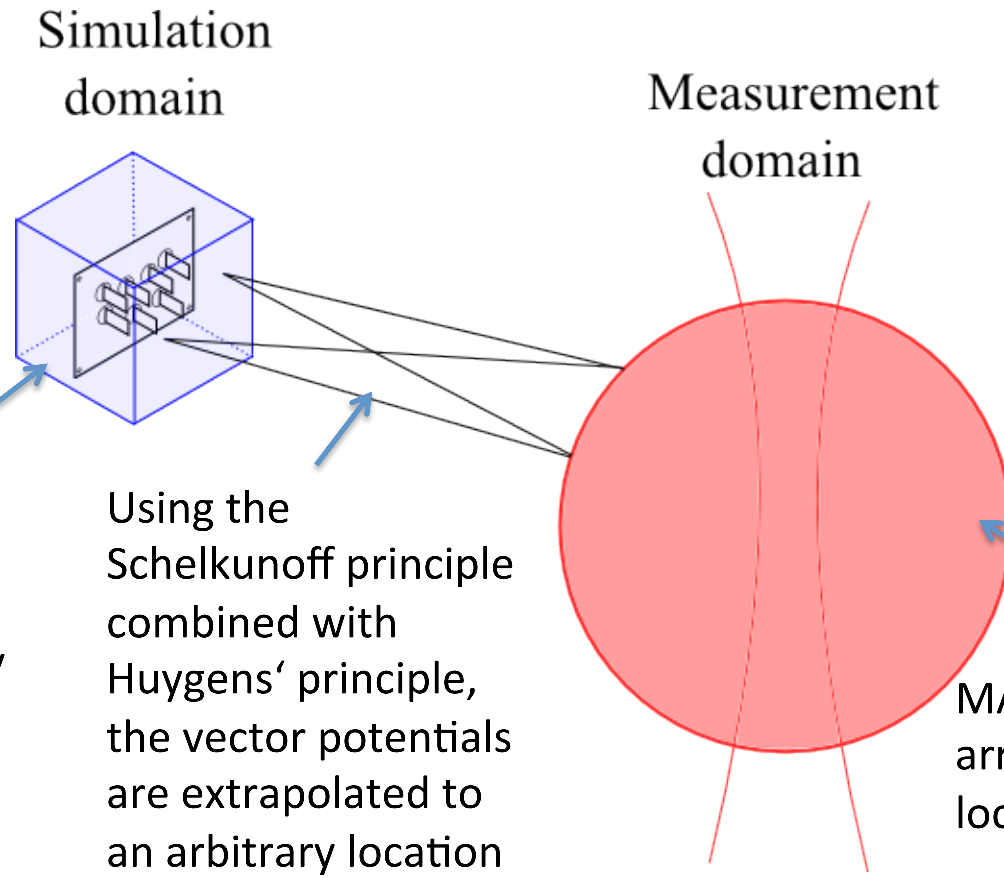

Detailed full wave simulation of the array over a small domain

Using the Schelkunoff principle combined with Huygens' principle, the vector potentials are extrapolated to an arbitrary location

MAST density cut off, or array measurement location

Future developments for SAMI

- Dual polarisation planar "sinuous" antennas
- Very stable phase centre
- Planar PCB antenna, avoids 3D field scattering effects.
- Cavity backed to control backwards pointing lobes

Research Councils UK Energy For a Low Carbon Future
EPSRC Engineering and Physical Sciences Research Council
UNIVERSITY of York
Durham University
CCFE CULHAM CENTRE FOR FUSION ENERGY

Outline

- Introduction and motivations – S. J. Freethy
  - Introduction to SAMI
  - Introduction to EBW emission
  - Results from MAST
- Reflectometry and backscattering – D. Thomas
  - Multiple refelctometers
  - Backscattering and doppler shifts
- Technical developments and upgrade – J. Brunner
  - FPGAs
  - The SAMI digitiser
  - FPGA/GPU data “real-time” data processing

Active Probing on SAMI

2 Active Probing Antennas

8 Receiving Antennas

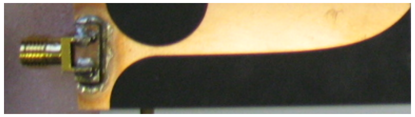

2cm

6cm

- SAMI can actively probe the plasma with two different IF frequencies (10,12 MHz) simultaneously

- The back scattered signals are then received by the 8 receiving antennas

- This can be done for 16 different frequencies 10-35GHz

Reflectometry using SAMI

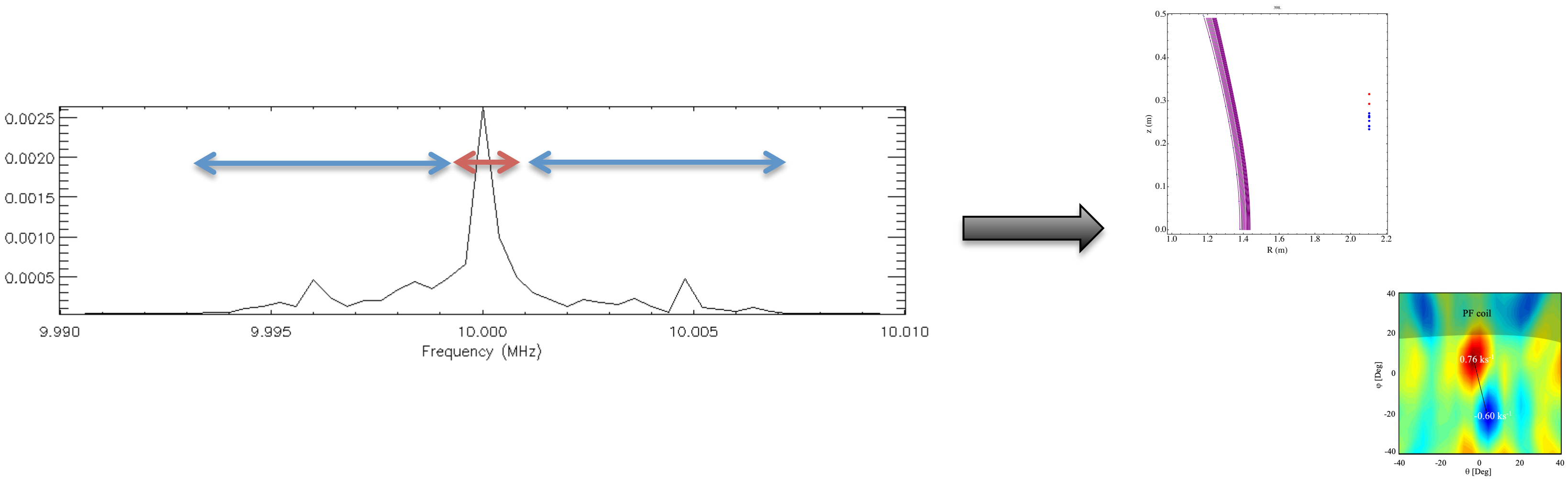

- Use a very small part of the IF frequency spectrum for reflectometry
- This is how it is possible to carry out passive and active imaging at the same time

Reflectometry using SAMI (cont'd)

- Having 2 active probing antennas and 8 receiving antennas means that we measure 16 different phases

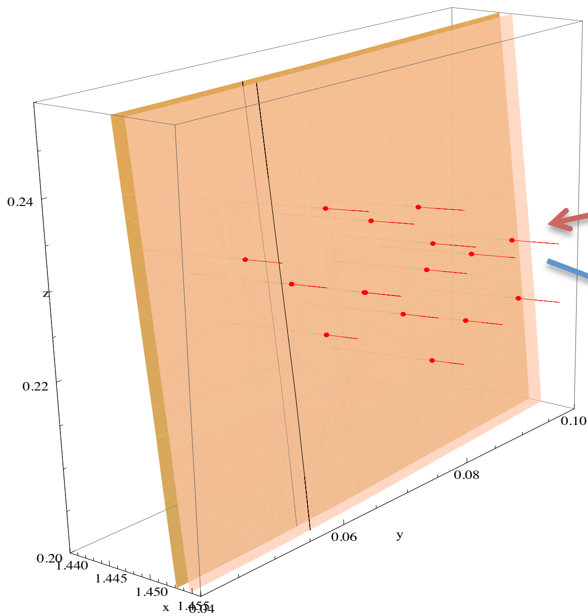

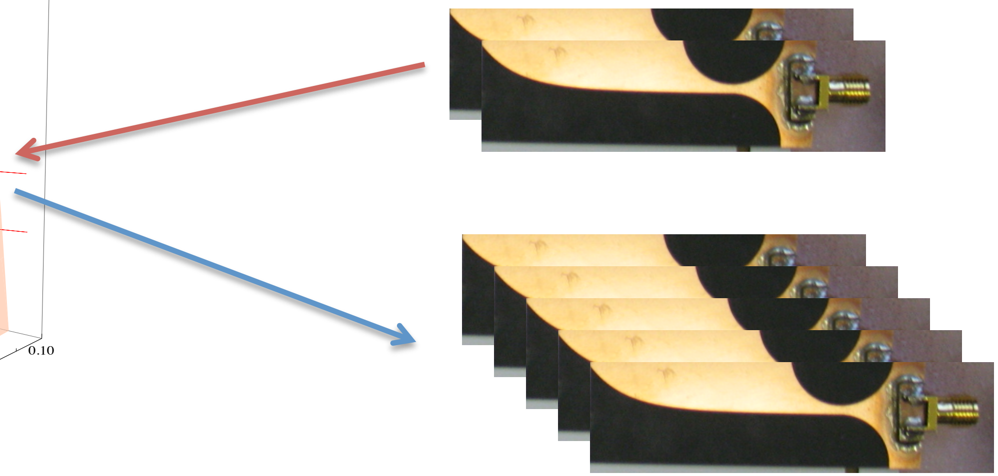

Reflectometry fitting proceedure

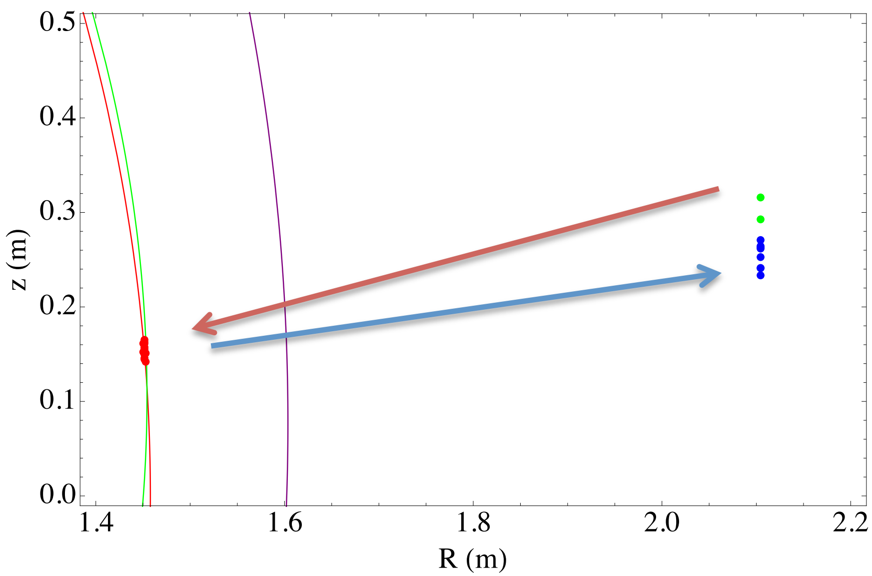

$x = [R - b + (a + b \cos \theta) \cos(\theta + \delta \sin \theta)] \cos \phi$
$y = [R - b + (a + b \cos \theta) \cos(\theta + \delta \sin \theta)] \sin \phi$
$z = z_0 + \kappa a \sin\theta$

- Using the differences in the phases we numerically minimize a function until we have a best fit
- This fitting proceedure has been tested on synthetic data
- Applying this fitting proceedure to SAMI data is ongoing

L-mode 98ms into MAST shot #27246

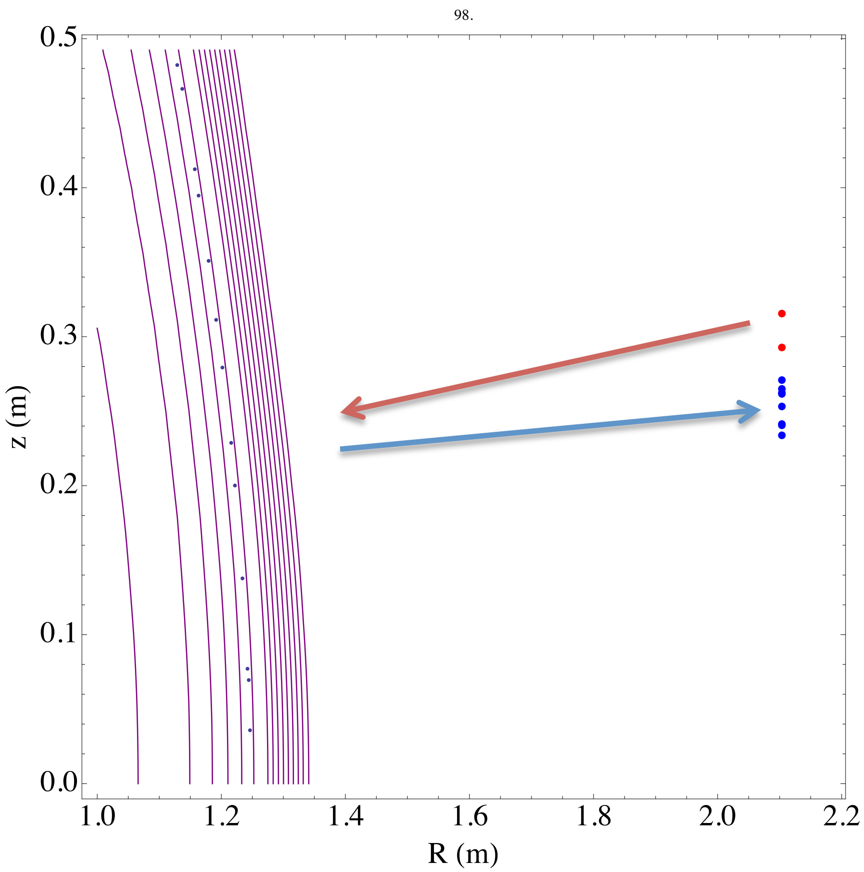

- The black dotted line represents the LCFS as calculated by EFIT
- The plasma density data is generated by Thomson Scattering along the mid-plane coupled to flux surfaces calculated by EFIT
- The red and blue dots represent the emitting and receiving antennas respectively.
- The purple surfaces represent contours where the plasma frequency is equal to one of the SAMI imaging frequencies.

H-mode 359ms into MAST shot #27246

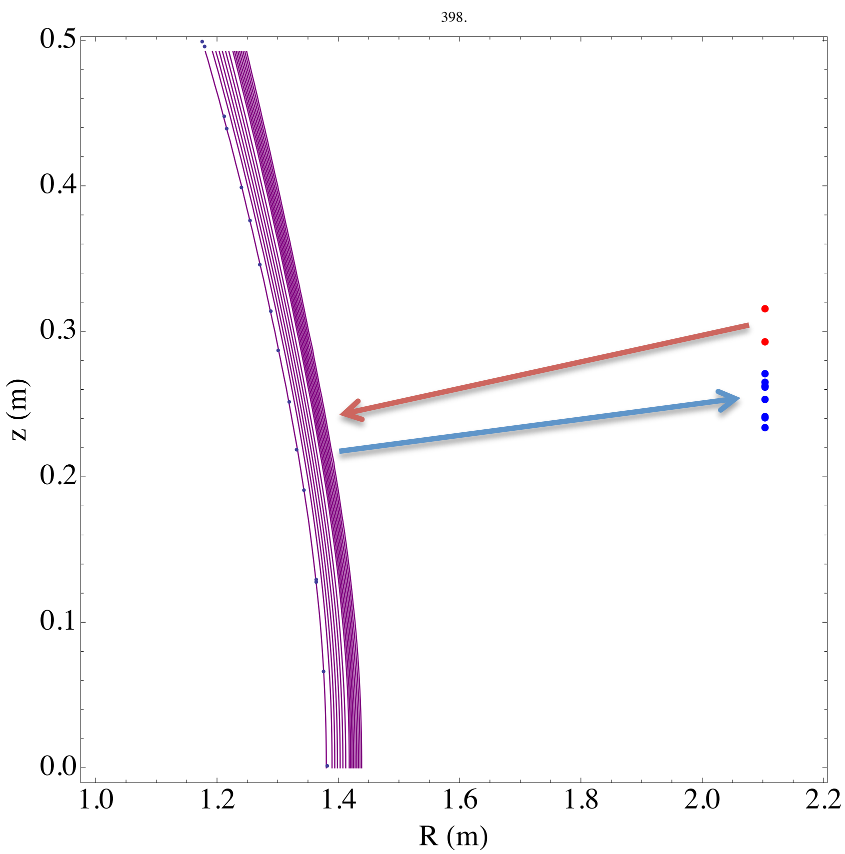

- We see that in H-mode all of the reflection surfaces are bunched up in the edge region
- This means we could get density measurements with a spatial resolution of ~3mm in the pedestal during H-mode.
- The accuracy at which we will be able to make these measurements is yet to be determined.

Accuracy of fitting

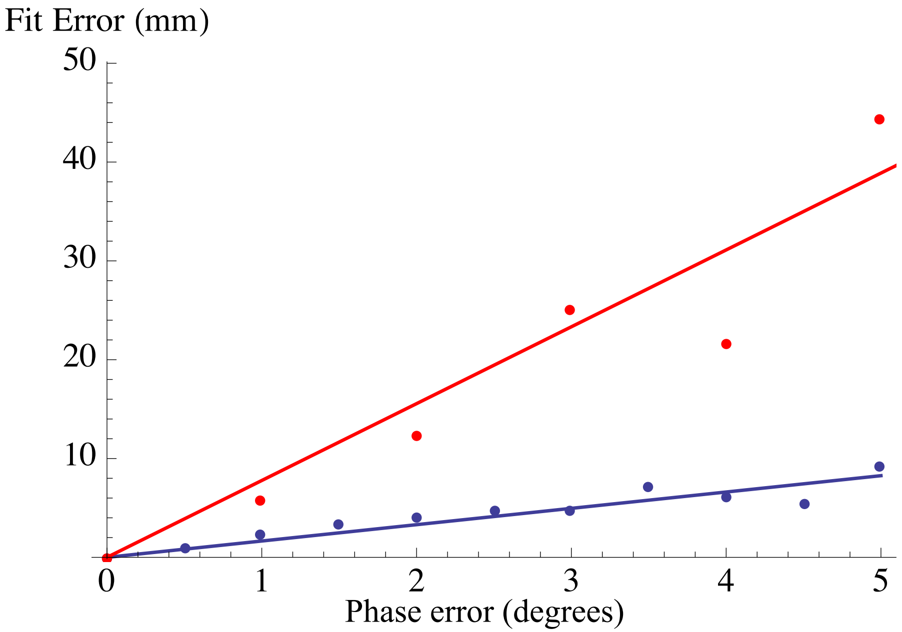

- A 2nd Active probing antenna has already been added to SAMI and a third could potentially be added in the future

- Very accurate pedestal density measurements could potentially be made

Doppler Reflectometry test setup

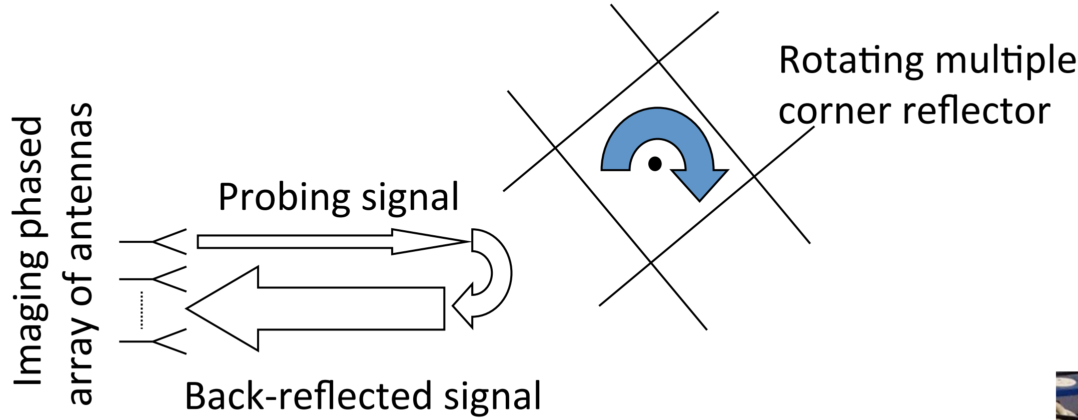

Rotating corner reflector
was used in calibration

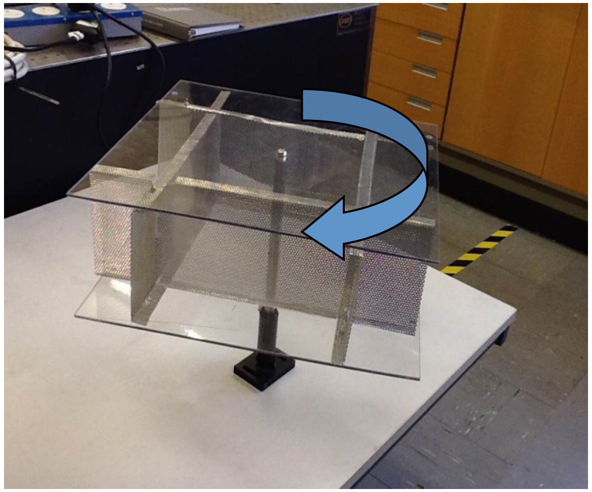

Doppler test setup results

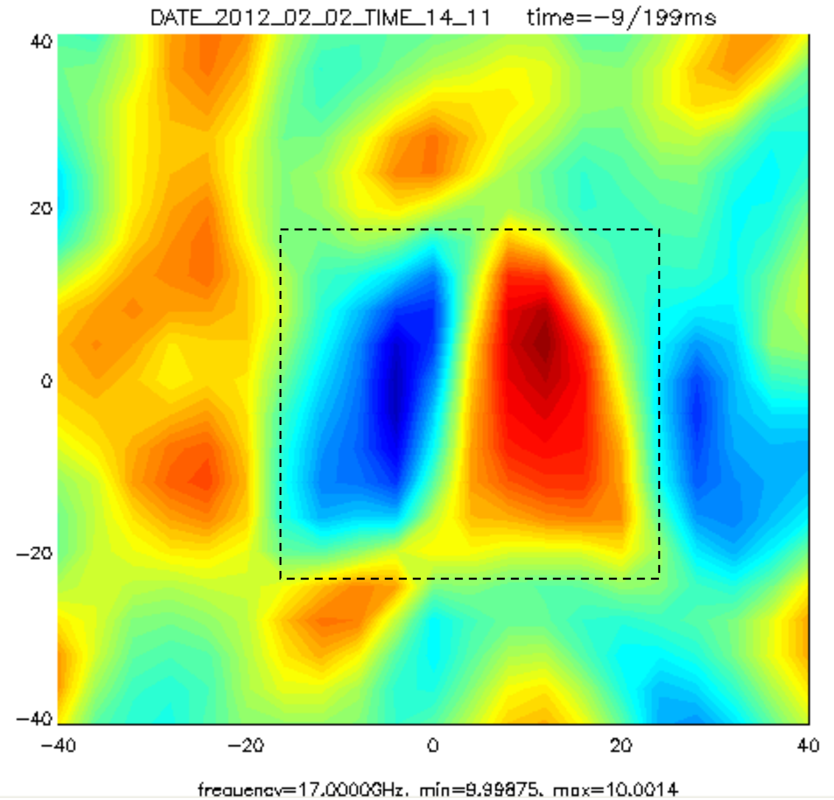

- Here we show a beam formed image of the rotating mesh at 17GHz time integrated over 200ms
- Red and blue shifted signals are apparent in the spatial locations we would expect.
- The amount of Doppler shift observed is ±250Hz which corresponds to a rotation rate of 3 rotations/sec consistent with the rotation speed used.

Plasma results

13GHz

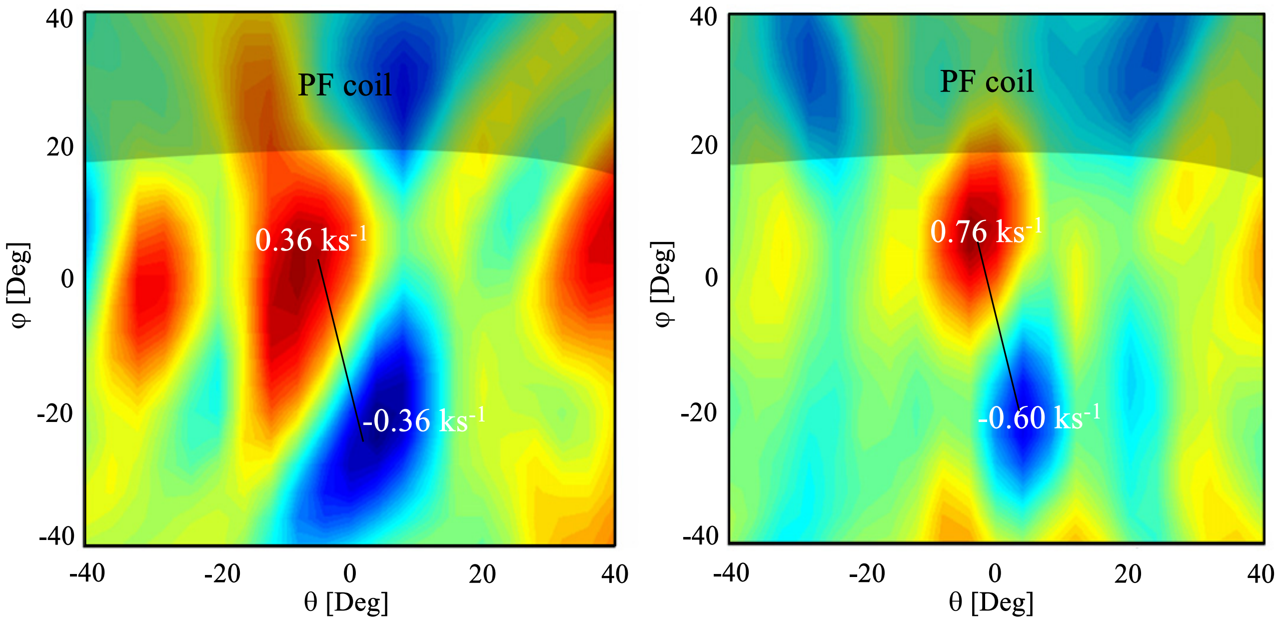

16GHz

- Images averaged over 10ms at 13 and 16GHz respectively.

- The spatial structure in the Doppler shift as the observed radiation is predominantly Bragg backscattered radiation from plasma turbulent structures aligned along the magnetic field.

L-mode spontaneous rotation

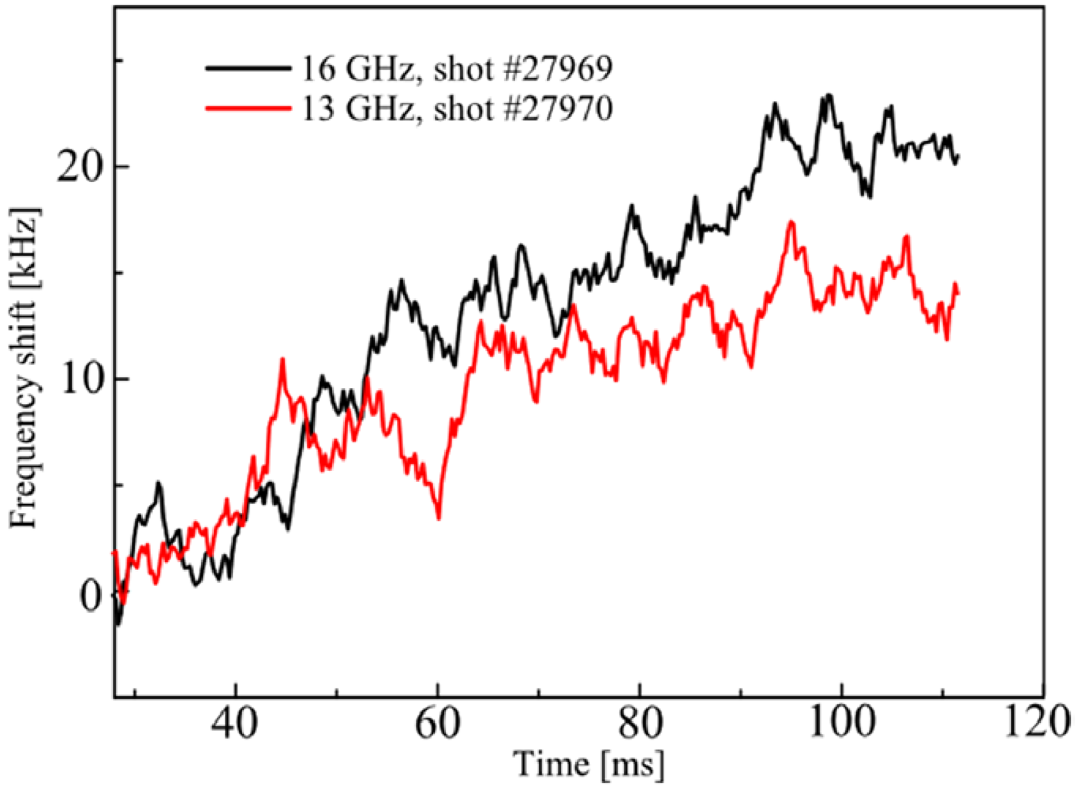

- Doppler shift as a function of time for 13 and 16 GHz.
- 16GHz is reflected from a deeper layer in the plasma.
- The 16 GHz layer is accelerated to a higher rotation velocity.

Coherent structures in Doppler Spectrum

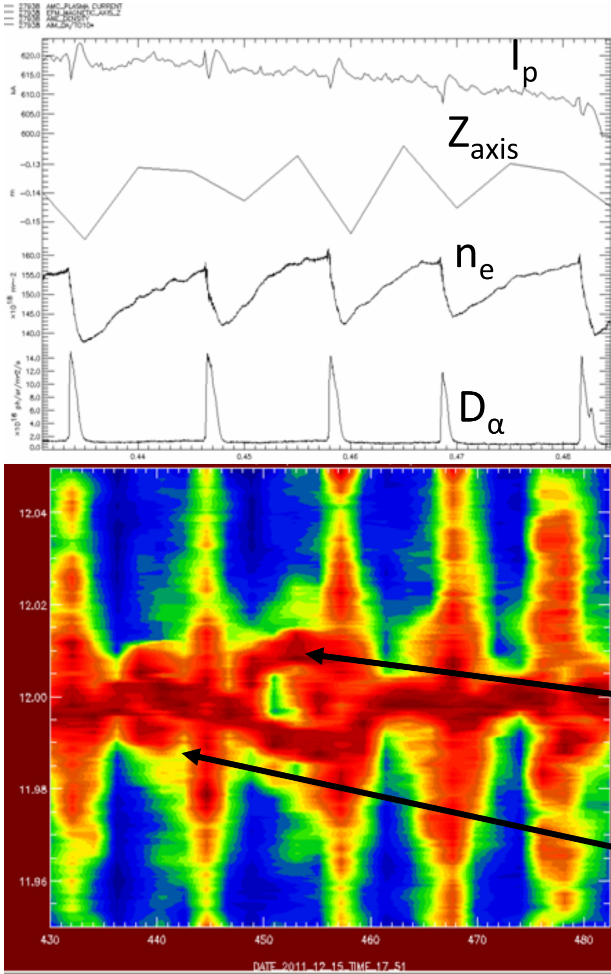

- Doppler back scattered (DBS) spectra plotted against time illustrate dynamics during and in between ELMs

- Coherent structures visible during ELMS

Coherent structure destroyed by ELM

Coherent structure collapsed itself

Aims on NSTX-U using active probing

- Make high resolution density measurements in the edge region of NSTX-U plasma. Plasma ~70cm away on MAST, ~15cm away -NSTX-U relative phase difference larger. This will aid reflectometry.

- Obtain Doppler maps of NSTX-U plasma

- Resolve coherent MHD structures using the spectrum of Doppler back scattered signals

Outline

- Introduction and motivations – S. J. Freethy
  - Introduction to SAMI
  - Introduction to EBW emission
  - Results from MAST
- Reflectometry and backscattering – D. Thomas
  - Multiple reflectometers
  - Backscattering and Doppler shifts
- Technical developments and upgrade – J. Brunner
  - FPGAs
  - The SAMI digitiser
  - FPGA/GPU data “real-time” data processing

Fast digitization for SAMI

- SAMI strongly dependent on synchronized high speed data acquisition across multiple channels
- At the same time variable configurations, i.e. active probing & passive imaging
- FPGAs enable high speed data acquisition for high bandwidth whilst allowing reconfiguration

[1] Shevchenko, V. F.; Vann, R. G. L.; Freethy, S. J. & Huang, B. K.
"Synthetic aperture microwave imaging with active probing for fusion plasma diagnostics"
Journal of Instrumentation, **2012**, *7*, P10016

FPGA basics – the fabric

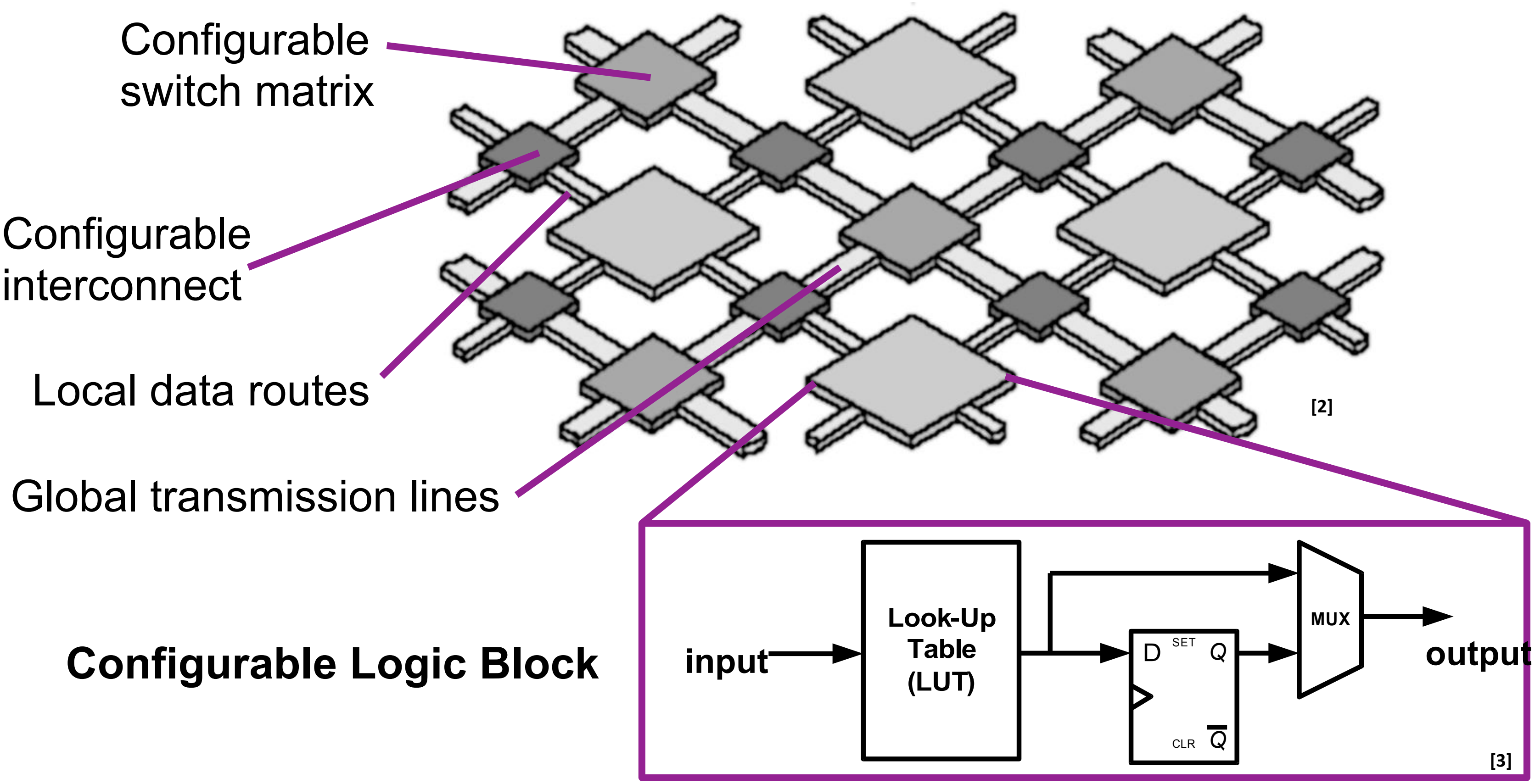

[2] "Introduction to Programmable Logic"; J. Coughlan.; RAL Technology Department, Lecture series 2007

[3] "Computer Architecture I – Laboratory Exercises Background and Introduction to FPGAs"; Konstantinos Tatas; Lecture series

FPGA basics – the CLB

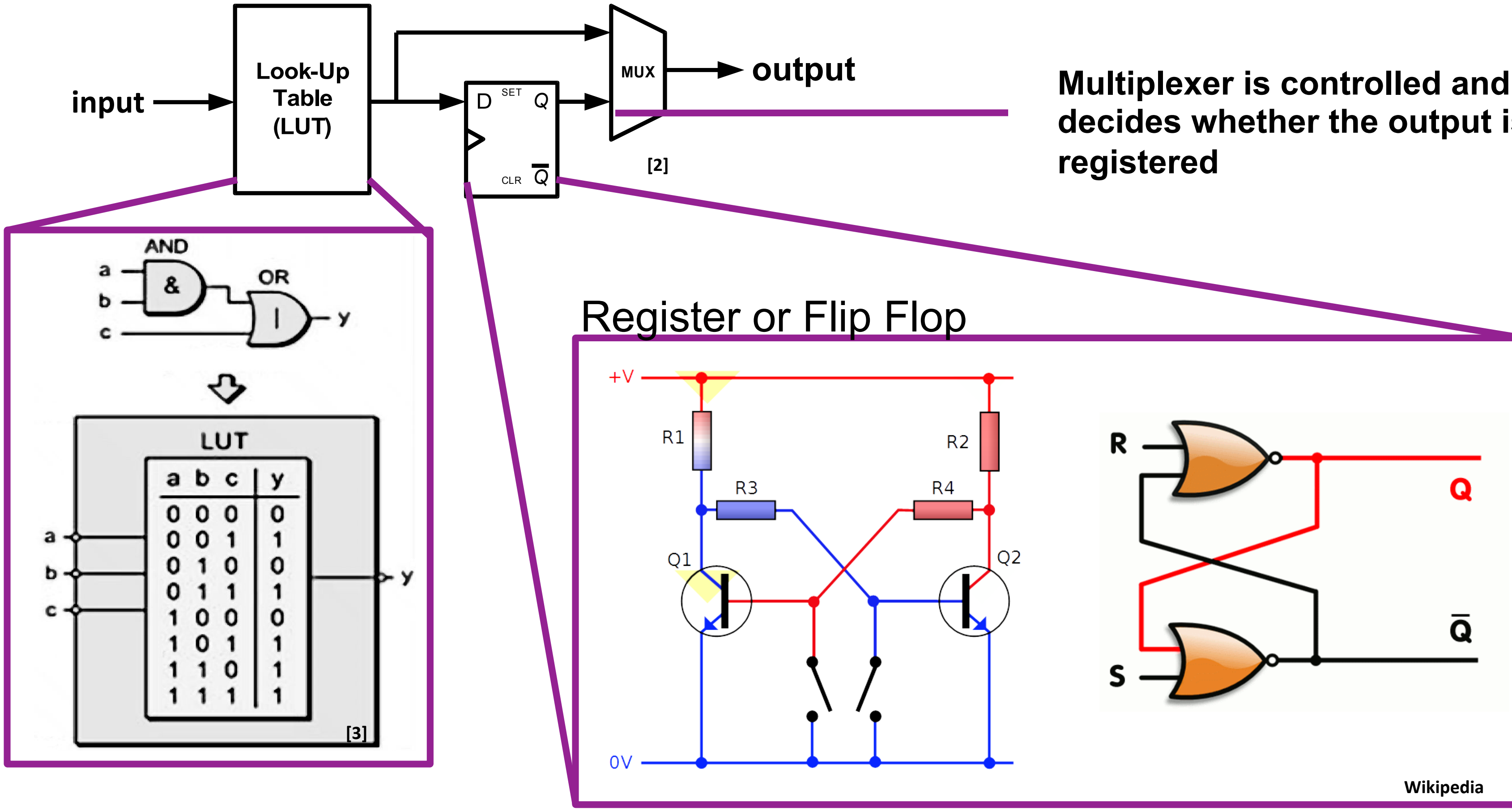

Multiplexer is controlled and decides whether the output is registered

[4] "Computing Performance Benchmarks among CPU, GPU, and FPGA"; Cullinan, C. and Wyant, C. and Frattesi, T. and Huang, X.; MathWorks; Apr 2012; E-project-030212-123508

FPGA basics – features

- In modern FPGAs the fabric has additional specialized blocks to enhance performance, i.e.

  - Block-RAM elements(BRAM)
  - Fast general purpose DSPs for multiplication etc.
  - Fast transceiver pins for high speed data transmission
  - Specialized delay blocks for timing
  - Dedicated Clock generation blocks

FPGA integration in SAMI

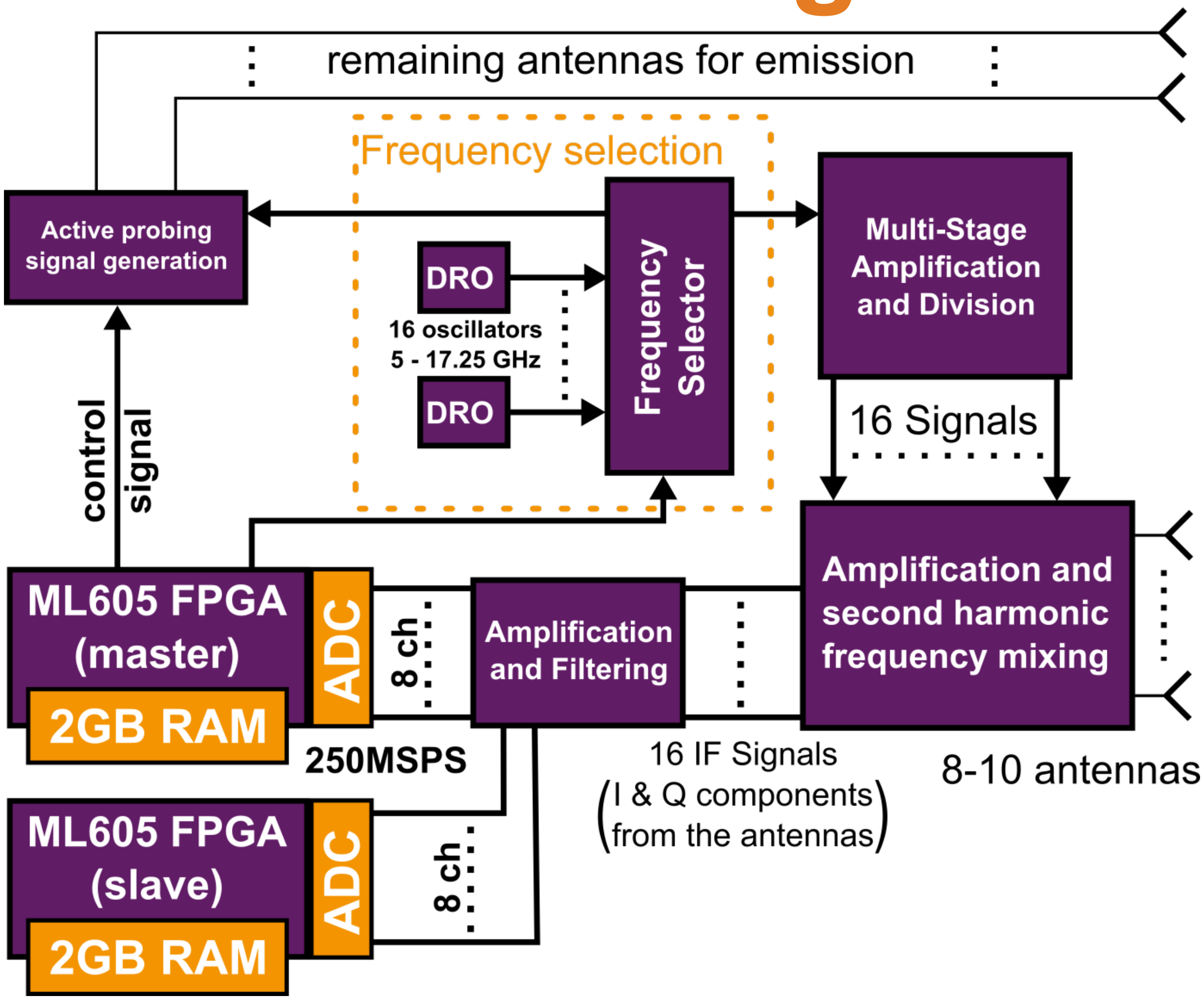

- FPGAs select frequencies from Local Oscillators (set before shot)
- FPGAs provide upconversion signal for active probing
- Currently FPGAs sample at 250MSPS with 14bit
  - 4GB of raw data on 500ms MAST shots
- running Linux on the FPGAs allows us to change the operation mode between shots

FPGA clock synchronization

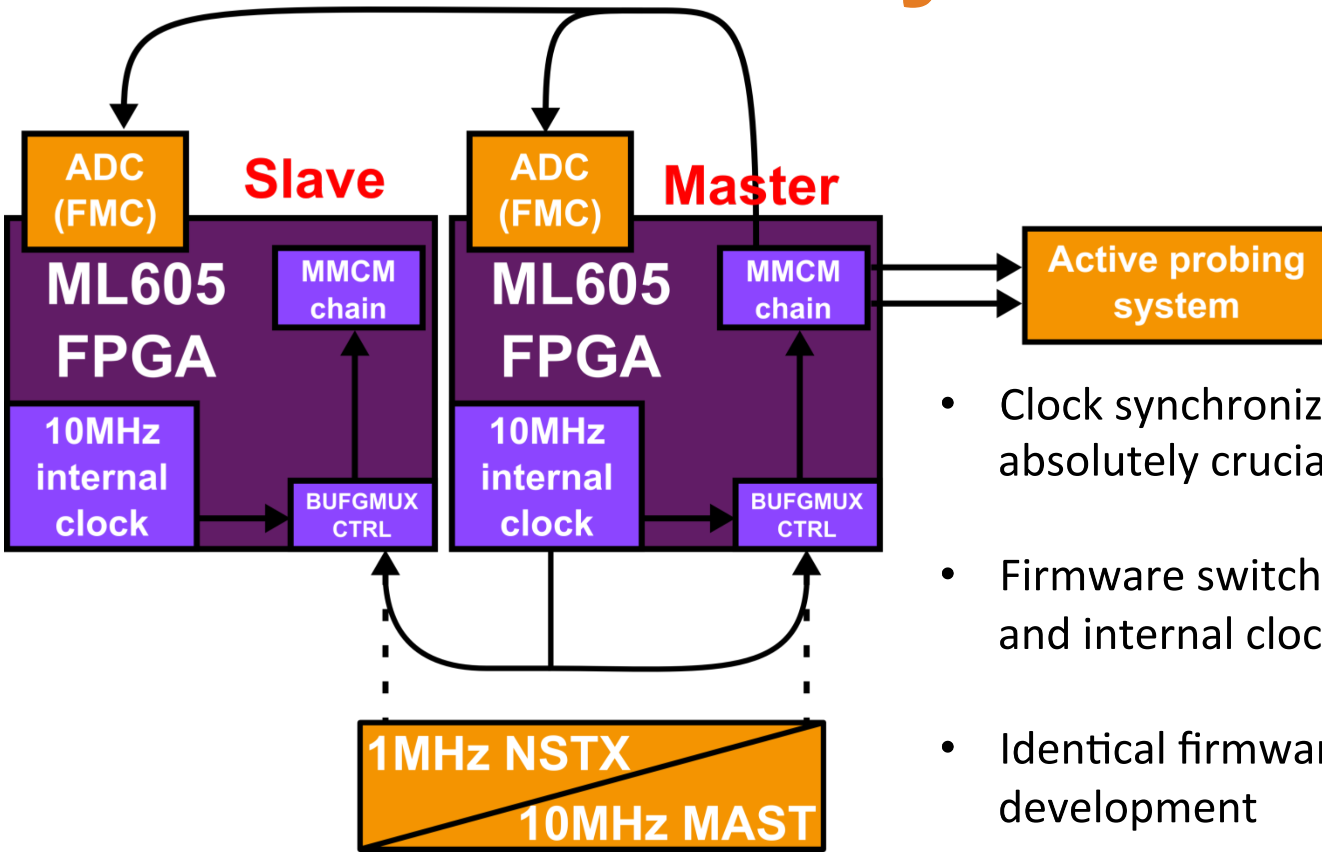

- Clock synchronization across boards is absolutely crucial for SAMI to work
- Firmware switches between an external and internal clock reference
- Identical firmware on both boards eases development
- Due to insufficiencies in reference clocks a board currently supplies the reference

FPGA setup on NSTX

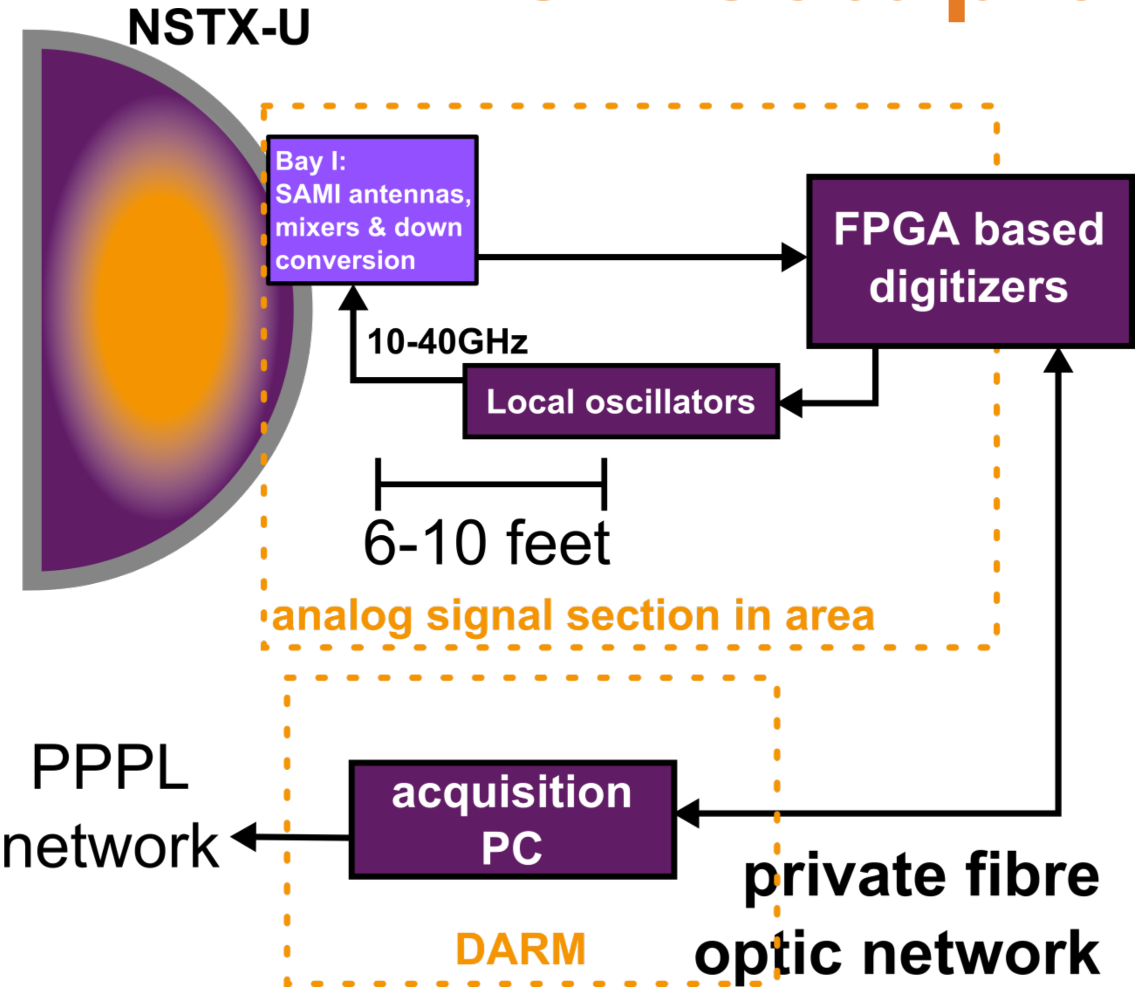

- Antenna rack with mixers for down conversion are placed directly on the rack

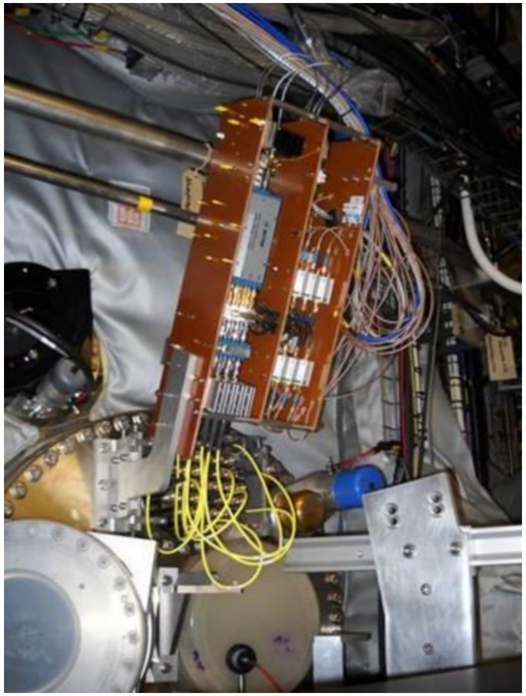

FPGA setup on NSTX

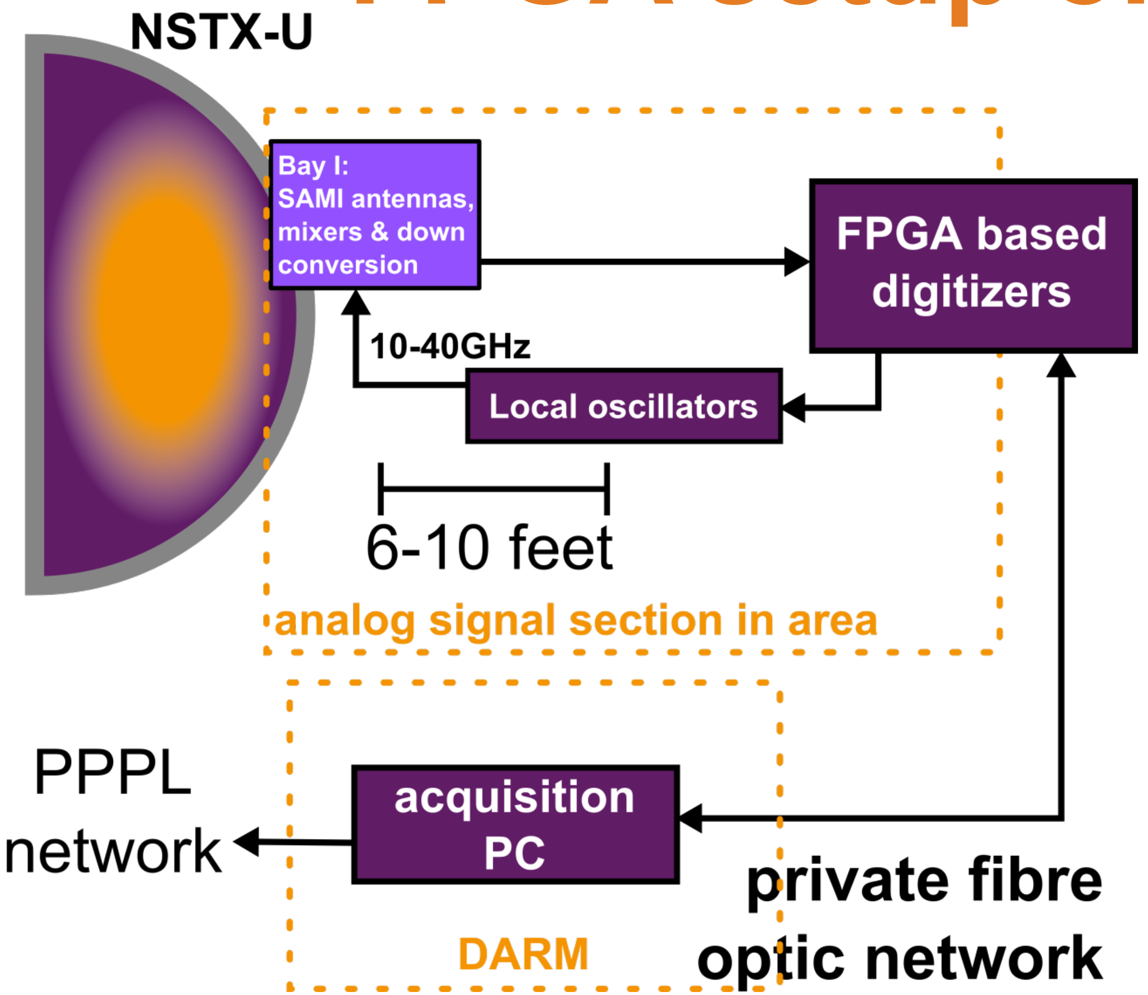

- Antenna rack with mixers for down conversion are placed directly on the rack
- Local oscillators have to stay close to the mixers
- FPGAs have a private fibre optic 100Mbit network with acquisition PC to download data and upload firmware
- The FPGA system is controlled via a webpage based on the acquisition PC

Moving SAMI forward: new challenges

- Currently SAMI collects 4GB of data per 500ms shot, which barely fits onto the FPGAs without the capability of upgrading the memory capacity
- Bypassing all security measures transfer of data from the FPGAs currently takes 2-3min, however the transmission is not fully reliable
- Processing of that data currently takes about 15-20min: more than the avg. time between MAST shots
- Both NSTX-U and MAST-U plan on operating multiple seconds and hence will require semi-continuous acquisition and thus data streaming with faster processing
- Limits in the currently employed system force us to completely redesign data transfer and processing

The future of SAMI

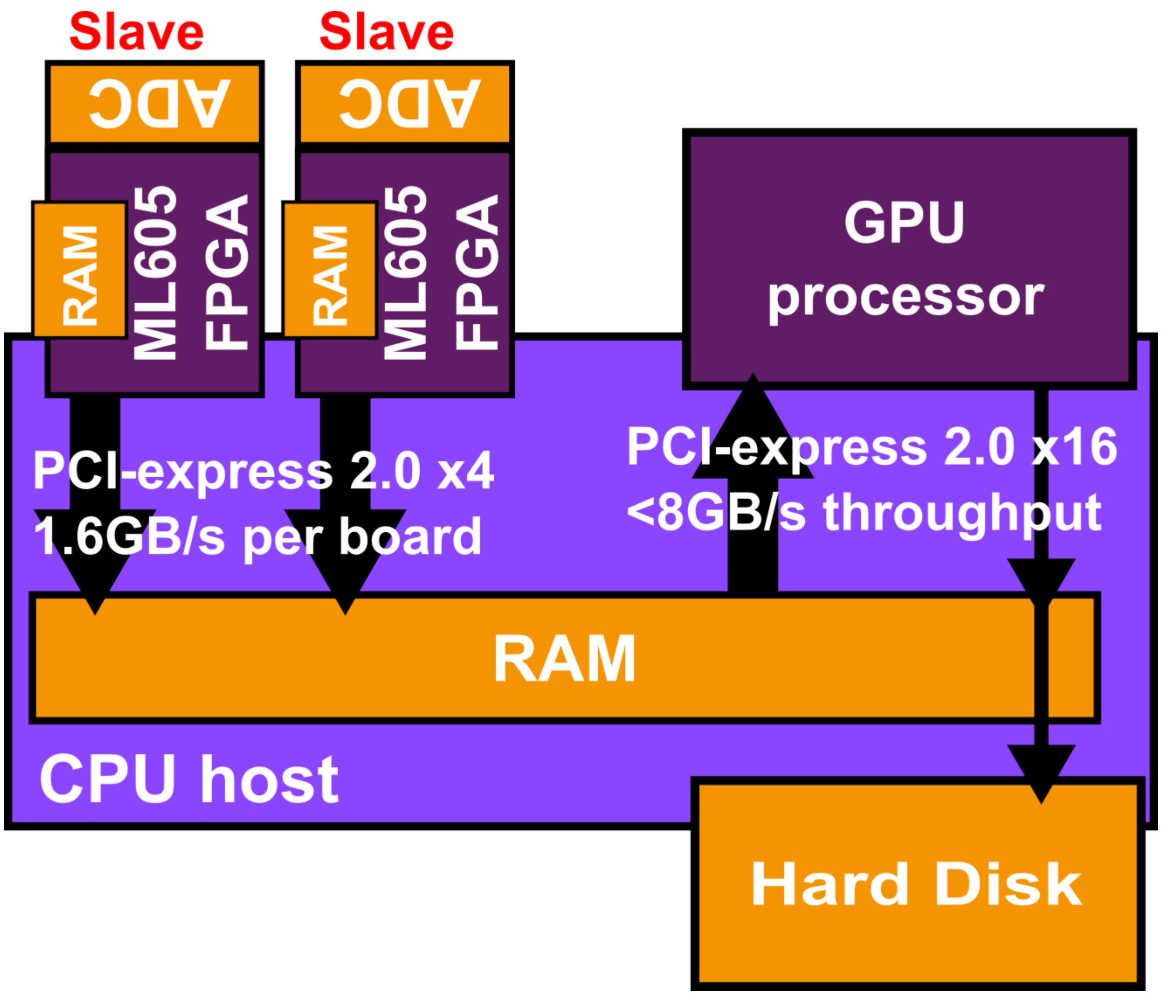

- Utilizing on board PCIe connectors transfer time could be reduced to seconds
- Streaming data into CPU host RAM directly and processing it after each shot would significantly increase SAMI operation limits
- Using GPUs to process data on the fly would reduce storage requirements

GPU based processing
(work done by Joanne Chorley)

- Serial IDL based data evaluation takes longer than the time between shots on MAST
- Evaluation algorithm using beam forming is highly parallelizable and thus fit for GPUs
- Main problem for the GPU is memory and transfer time as the data amount doubles on read in and temporarily grows up to triple the size during processing
- Parallelizing the code and "outsourcing it to a GPU brought significant speed up

	Total Algorithm Time[s]	Reading data from Memory [s]	Compute Time(s)
IDL	1038.378	128.32 *	910.058 *
C (serial code)	464.55	88.160 *	376.39 *
CUDA (NVIDIA K40)	17.4238	11.65	5.7748

An FPGA-GPU tandem

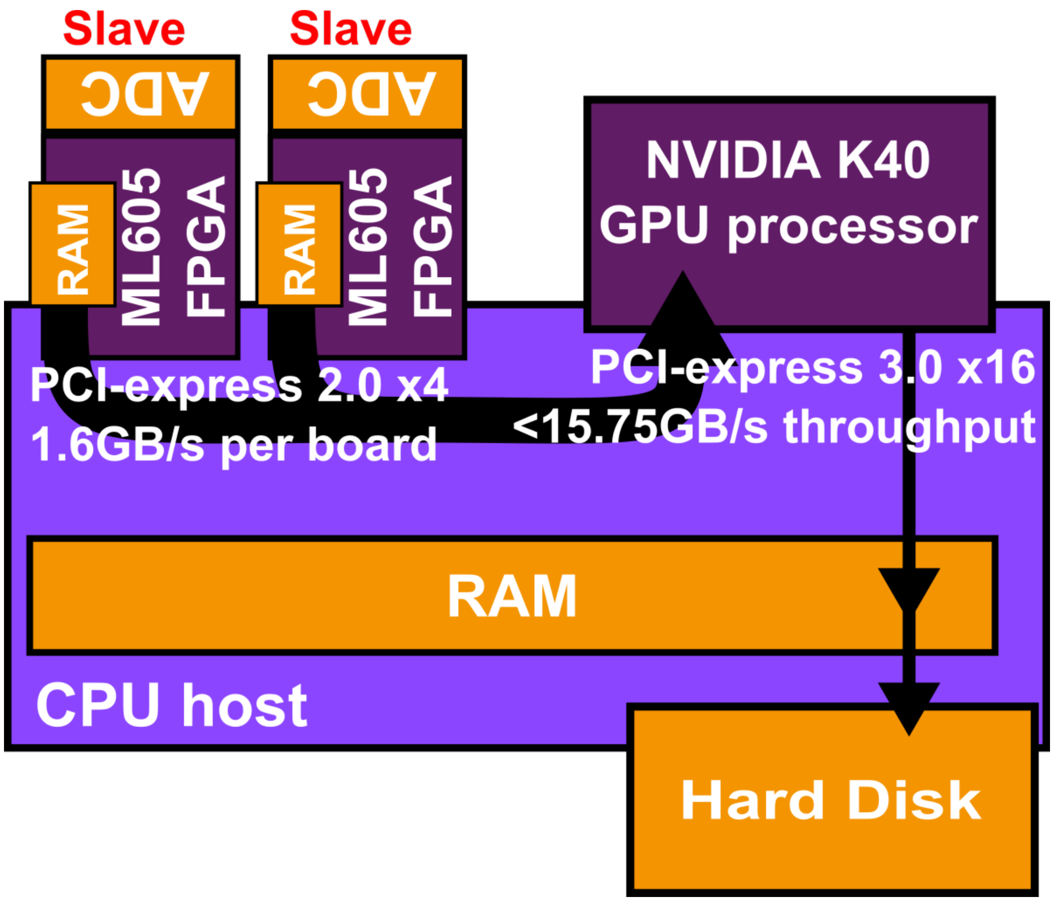

- To achieve maximum data transmission between GPU and FPGAs direct streaming of data between the devices is beneficial
- Treating FPGA memory as an extension to the GPU memory can bypass the CPU host and utilize the maximum speed of the PCIe bridge
- Saving only a fraction of the RAW data plus the processed data should decrease the amount of data by a factor of 2000